# Cardiovascular Molecular Imaging[1]

Joseph C. Wu, MD, PhD
Frank M. Bengel, MD
Sanjiv S. Gambhir, MD, PhD

The goal of this review is to highlight how molecular imaging will impact the management and improved understanding of the major cardiovascular diseases that have substantial clinical impact and research interest. These topics include atherosclerosis, myocardial ischemia, myocardial viability, heart failure, gene therapy, and stem cell transplantation. Traditional methods of evaluation for these diseases will be presented first, followed by methods that incorporate conventional and molecular imaging approaches.



[1] From the Department of Medicine, Division of Cardiology (J.C.W.), Department of Radiology, Molecular Imaging Program at Stanford (J.C.W., S.S.G.), and Bio-X Program (S.S.G.), Stanford University, 300 Pasteur Dr, Edwards Bldg R354, Stanford, CA 94305-5344; and Department of Nuclear Medicine, Johns Hopkins University, Baltimore, Md (F.M.B.). Received January 25, 2006; revision requested March 24; revision received April 7; final version accepted June 1. **Address correspondence to** J.C.W. (e-mail: *joewu@stanford.edu*).

Molecular imaging is a rapidly advancing biomedical research and clinical discipline. Compared with traditional in vitro tissue culture and in vivo animal studies, molecular imaging allows noninvasive, quantitative, and repetitive imaging of targeted biological processes at both the cellular and subcellular levels within a living organism (1). This kind of imaging provides an extremely powerful technique with numerous applications, such as the monitoring of endogenous transcriptional regulation, analysis of gene transfer, tracking of tumor cell survival, screening for transgenic animal phenotypes, and expediting of drug discovery (2). Although the primary focus traditionally has been in the field of cancer biology, molecular imaging approaches have now been extended to several cardiovascular-related applications.

The goal of this review is to highlight how molecular imaging will impact the management and improved understanding of the major cardiovascular diseases that have substantial clinical impact and research interest. These topics include atherosclerosis, myocardial ischemia, myocardial viability, heart failure (HF), gene therapy, and stem cell transplantation. Traditional methods of evaluation for these diseases will be presented first, followed by methods that incorporate conventional and molecular imaging approaches. Conventional cardiovascular imaging focuses on obtaining anatomic, physiologic, or metabolic information and includes modalities such as echocardiography, magnetic resonance (MR) imaging, computed tomography (CT), single photon emission computed tomography (SPECT), and positron emission tomography (PET).

Although echocardiography, MR imaging, and CT typically are used to evaluate anatomic structures of the heart, they have limited capabilities in the assessment or visualization of physiologic and metabolic processes. Conversely, SPECT and PET can be used to evaluate physiologic and metabolic characteristics but are limited in their capability for visualization of anatomic structures. By using standard anatomic imaging modalities combined with molecular imaging technologies such as SPECT and PET, we now have the potential to detect disease processes at the anatomic, physiologic, metabolic, and molecular levels and, thereby, allow *(a)* earlier detection of diseases, *(b)* objective monitoring of therapies, and *(c)* better prognostication of disease progression (3).

## Atherosclerosis

Atherosclerosis is a dynamic multifactorial disease of the arterial wall. Although it generally involves the entire vascular system, cardiovascular manifestations are found most frequently and ultimately result in clinically overt coronary artery disease (CAD). A variety of factors contribute to development and progression of atherosclerosis. Dysfunction of the endothelium, which maintains vascular homeostasis by regulating vascular tone, smooth muscle cell proliferation, and thrombogenicity, is thought to be the earliest step in the development of CAD. The endothelial dysfunction results in the imbalance of vascular regulatory mechanisms to cause damage to the arterial wall (4). Inflammation, macrophage infiltration, lipid deposition, calcification, extracellular matrix digestion, oxidative stress, cell apoptosis, and thrombosis are among further molecular mechanisms that contribute to plaque development and progression (5) (Fig 1a, 1b).

In the past, invasive coronary angiography has been the only diagnostic procedure that could be used to identify coronary atherosclerosis. The reduction of the vessel lumen caused by stenosis is used as an indicator of the presence of plaques and allows assessment of the extent and severity of occlusive CAD. Advances in CT and MR imaging technology have led to the development of algorithms for noninvasive contrast material–enhanced angiography by using these techniques (6). These approaches are characterized by high negative predictive values, but their diagnostic accuracy, especially for the assessment of smaller distal parts of the coronary arterial tree, is still limited at present.

Although angiography still serves as a key test in the management of symptomatic CAD, several clinical observations have emphasized the need for a more detailed analysis of the structure and biology of atherosclerotic plaques. First, epidemiologic observations have shown that a large proportion of people who suffer a sudden cardiac event (acute ischemic syndrome or sudden cardiac death) have no prior symptoms (7). Second, it has been found that acute coronary syndromes often result from plaque rupture at sites with no or only modest luminal narrowing at angiography (8) (Fig 1a). Vascular remodeling, which consists of atherosclerosis-associated morphologic and biologic changes of the vessel wall without substantial stenosis, often has occurred at such sites (9). Therefore, there is considerable demand for diagnostic procedures that go beyond assessment of the vessel lumen to identify rupture-prone vulnerable plaques as the most frequent cause of sudden cardiac events (5).

As a consequence, several methods have been developed in recent years to provide detailed information about vessel wall and plaque morphology. Intravascular ultrasonography (US) is an invasive technique that allows assessment of vessel wall thickness and structure (10). In addition, optical coherence tomography has been introduced as another invasive technique that provides images of vessel wall morphology at almost histologic quality (11). Finally, MR imaging approaches also have been developed, and these approaches allow noninvasive characterization of the ves-

**Published online before print**
10.1148/radiol.2442060136

**Radiology 2007;** 244:337–355

**Abbreviations:**
CAD = coronary artery disease
FDG = fluorine 18 fluorodeoxyglucose
FHBG = 9-(4-[18F]fluoro-3-hydroxymethylbutyl)guanine
HF = heart failure
ICD = implantable cardioverter defibrillator
MI = myocardial infarction
MIBG = *m*-iodobenzylguanidine
VEGF = vascular endothelial growth factor

Authors stated no financial relationship to disclose.

sel wall (12). Some studies have shown that CT angiography allows additional assessment of plaque attenuation (13). The goal of these techniques is to identify vascular remodeling and describe plaques with regard to specific criteria of vulnerability, such as a thin fibrous cap and a large lipid core.

At least as important as its morphology, however, is the biology of a plaque (Fig 1b). Inflammation is a key feature of active, rupture-prone plaques, which can be identified invasively by using thermography (14). Plaque inflammation also may be identified noninvasively by using nuclear imaging with fluorine 18 ($^{18}$F) fluorodeoxyglucose (FDG) or other markers of inflammatory activity (15). Further molecular features of unstable plaques, which have been targeted by specific probes, are macrophage infiltration (16,17), proliferating smooth muscle cells (18), matrix metalloproteinase activation (19), apoptosis of macrophages and smooth muscle cells (20,21), oxidative stress (22), and proangiogenetic factors (23) (Table 1).

Most of these biologic imaging techniques are at present still limited to experimental settings, but the increasing number of upcoming approaches and of research groups active in the field will help for rapid future clinical establishment. Hybrid imaging systems such as PET/CT and SPECT/CT cameras are anticipated to contribute substantially to a breakthrough in clinical identification of vulnerable plaques, because these systems allow combined assessment of morphology and biology of vascular structures at sufficiently high spatial resolution (Fig 1c).

## Myocardial Ischemia

As mentioned previously, atherosclerosis ultimately progresses to clinically overt CAD. In the treatment of clinical CAD, a paradigm change has occurred in recent years. It is increasingly emphasized that the decision for invasive work-up and intervention cannot be based on symptoms and morphologic detection of coronary stenoses alone. Functional tests allow accurate identification of the presence, extent, and severity of myocardial ischemia, which is closely correlated to patient outcome. At present, detection of myocardial ischemia thus serves as a gatekeeper to coronary angiography and guides the clinician to choose interventional or medical therapy on the basis of individual cardiovascular risk (Fig 2).

The clinical usefulness of myocardial perfusion scintigraphy for diagnostic and prognostic evaluation of patients with suspected or known CAD is sup-

**Figure 1**

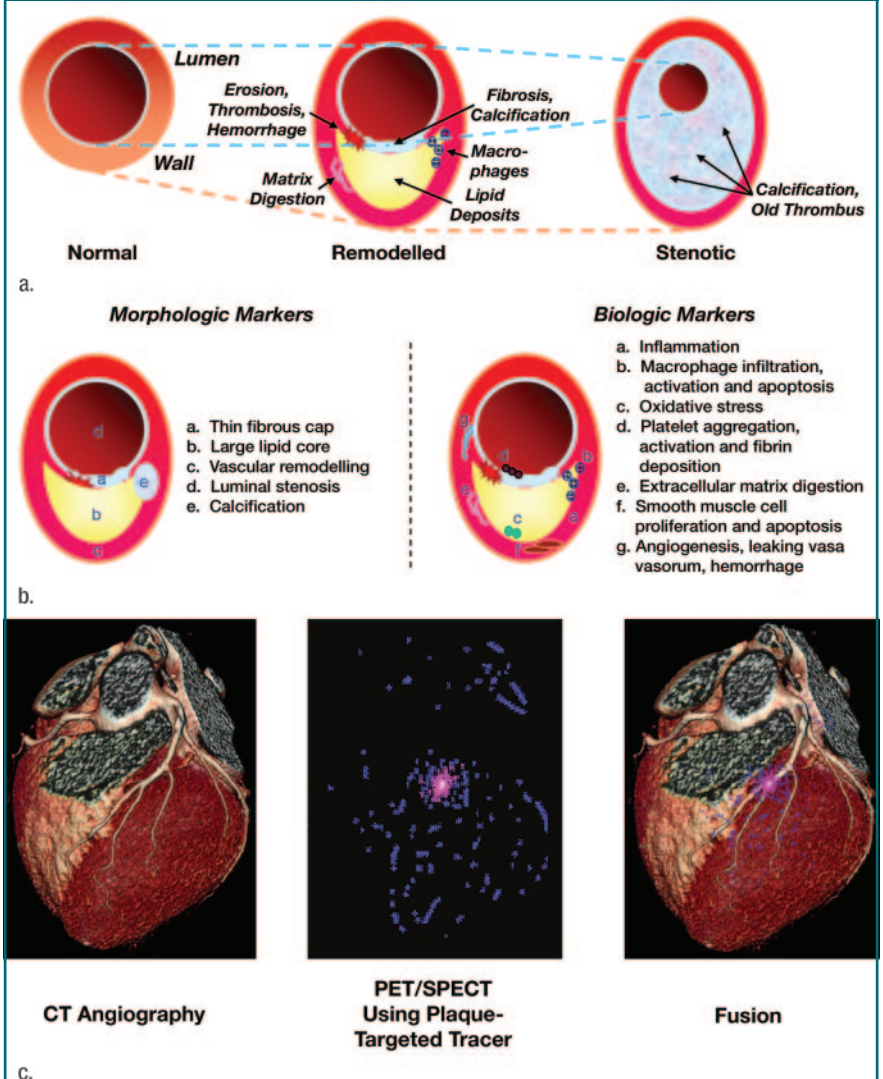


**Figure 1:** From atherosclerotic plaque biology toward molecular plaque imaging. **(a)** Atherosclerosis and vascular structure. Image shows development of expansive vascular remodeling, which may result in substantially increased vulnerability without luminal narrowing. Ultimately, changes lead to acute plaque rupture or to chronic stenosis with luminal narrowing (right). **(b)** Criteria of plaque vulnerability as targets for imaging. Image depicts morphologic and biologic features of vulnerable plaques, which are suitable targets for imaging approaches. **(c)** Future perspective in regard to multimodality imaging of plaque morphology and biology. Image highlights the potential of hybrid imaging technologies, which may allow noninvasive fusion of morphology from angiography with biology from nuclear imaging of plaque-targeted molecular probes (nuclear and fusion images are simulated).

ported by a large body of evidence. A normal myocardial perfusion scan can be used to rule out myocardial ischemia and is associated with a low cardiovascular event rate of less than 1% per year (24). Cardiac risk, and thus the benefit from invasive therapeutic strategies, increases in relation to the severity of myocardial ischemia and perfusion abnormalities (25,26). Noninvasive ischemia-guided strategies for diagnostic and therapeutic work-up of patients with CAD were shown to be cost effective in general (27). In addition, the importance of perfusion imaging for decision making has been demonstrated in specific situations, such as in acute coronary syndromes (28), after myocardial infarction (MI) (29), prior to noncardiac surgery, or in high-risk subgroups such as diabetic patients (30).

Nonnuclear imaging techniques for detection of myocardial ischemia are becoming increasingly available. These techniques have the advantage of no radiation exposure, but their diagnostic and prognostic usefulness is still less well established compared with perfusion scintigraphy. Echocardiography can be applied for detection of wall motion abnormalities during physical exercise (31) or dobutamine stimulation (32). Furthermore, contrast-enhanced echocardiography has been established for measuring perfusion with echogenic microbubbles (33). A promising approach to detection of ischemia is MR imaging. This technique is thought to be less dependent on patient conditions and observer experience. MR imaging can be effectively used for detection of ischemia-associated wall motion abnormalities during dobutamine stimulation (34) or for direct assessment of myocardial perfusion after a bolus injection of a gadolinium-based contrast agent at rest and during pharmacologic vasodilation (35). Although these nonnuclear methods are likely to grow in the future, it is thought that nuclear imaging will be pushed by the hybrid PET/CT and SPECT/CT cameras, which allow further refinement of functional cardiac assessment with measurement of myocardial perfusion, geometry, function, and coronary morphology within a single imaging session.

Assessment of ischemia by using measurement of perfusion and function will remain the method for stratification of patients with known CAD. Identification of ischemia-associated molecular alterations, however, may find a role in certain situations that are not yet possible through conventional assessment of perfusion and/or contractile function. Specific identification of myocardium that has previously been exposed to ischemia, but is now normally perfused, would be of considerable interest. An ischemic memory marker would allow identification of myocardium at risk in patients with acute coronary syndromes or extensive CAD. It may also provide insights into the clinical role of ischemic preconditioning, a cellular mechanism by which short episodes of ischemia and reperfusion result in an improved tolerance of prolonged ischemic episodes (36).

Annexin V is a protein that can be radiolabeled and that binds to phosphatidylserine, a molecule expressed on the cell surface during the early phase of apoptosis (programmed cell death). Recent studies have shown that annexin V uptake occurs not only in irreversibly damaged infarcted myocardium (37) but also temporarily in myocardium after reversible severe ischemia (38,39). These observations suggest that early phases of apoptosis are reversible and that annexin V may be used as a molecular marker to identify areas that have previously suffered severe ischemia but have not yet transformed to scar. Another approach for molecular imaging of ischemic memory is the application of the radiolabeled fatty acid analogue iodine 123 ($^{123}$I) β-methyl-*p*-iodophenylpentadecanoic acid. After episodes of ischemia, which result in a metabolic shift from fatty acids to glucose as the preferred substrate for energy production, regional uptake of this tracer seems to be reduced for a longer period of time (40).

**Table 1**

**Visualization of Biologic Features of Vulnerable Plaques**

| Molecular Mechanism | Probe | Imaging Method |
|---|---|---|
| Plaque inflammation | Thermography, FDG | Invasive, nuclear |
| Macrophage infiltration | Superparamagnetic iron oxide–labeled macrophages, radiolabeled monocyte chemoattractant protein 1 | MR imaging, nuclear |
| Apoptosis | Radiolabeled annexin V | Nuclear |
| Matrix degradation | Radiolabeled matrix metalloproteinase inhibitors | Nuclear |
| Angiogenesis | Labeled integrin ligands | Nuclear, MR imaging |
| Thrombosis | Labeled fibrin-binding peptides | Nuclear, MR imaging |
| Smooth muscle cell proliferation | Radiolabeled Z2D3 antibodies | Nuclear |

## Coronary Artery Disease

Another area of interest for targeted molecular imaging is to identify patients with CAD who have a high likelihood for ischemia-induced remodeling, a phenomenon that results in transition to HF. Early identification of such patients would allow prevention of the development of remodeling-associated ventricular dilatation and reduction of contractile function. Alterations of the cardiac sympathetic nervous system seem to play a critical role in left ventricular remodeling. Integrity of presynaptic sympathetic nerve endings can be identified by using radiolabeled catecholamines such as $^{123}$I–*m*-iodobenzylguanidine (MIBG). Researchers in several studies have identified innervation defects larger than perfusion defects in patients with CAD and after MI; these findings suggest that sympathetic neurons are more sensitive to ischemia than are myocytes (41,42).

An imbalance of autonomic signal transduction may contribute to the maladaptive process of postischemic remodeling. This idea has been suggested by investigators who observed acceler-

ated ventricular dilatation in patients with larger innervation defects that were indicated by reduced myocardial MIBG uptake (43). In addition to presynaptic innervation, postsynaptic receptor density can be evaluated by using PET and radiolabeled adrenergic receptor antagonists. Findings in a study showed that reduction of β-adrenergic density early after MI can be used to predict ventricular volumes at 6 months after the event (44); such results suggest that receptor-targeted imaging may be another approach to identify candidates for remodeling. Other molecular targets in the ischemic myocardium include integrins, a group of adhesion molecules that play a central role in angiogenesis. These can be identified with specific αvβ3-integrin–targeted radiotracers in vivo (45) and may allow assessment of postischemic recovery and angiogenesis therapy in the future (46). Finally, myocyte apoptosis is thought to be another relevant feature of remodeling that may be targeted by noninvasive molecular imaging although no detailed trials have been performed up to now.

## Myocardial Viability

It has been extensively documented that patients with poor left ventricular function and advanced multivessel CAD show improved clinical outcome after surgical revascularization (47–50). These patients may benefit most from revascularization, but the decision to proceed with interventional therapy is not an inconsequential one. Patients with severe ventricular dysfunction undergo coronary artery bypass graft surgery or percutaneous coronary intervention with a considerable risk of procedure-related morbidity and mortality (50). Hence, accurate methods to identify patients who will benefit most are required to justify the potential risks.

There has been increasing clinical awareness that contractile dysfunction in patients with CAD does not necessarily reflect the presence of scar tissue (51). In investigations of contractile reserve in the catheterization laboratory in the 1970s, reversibility of left ventricular dysfunction was described (52,53). Since then, several noninvasive imaging techniques have been developed to identify tissue viability in dysfunctional myocardium and to thereby determine which patients with ventricular dysfunction are the most appropriate candidates for revascularization (54).

Two major pathogenetic mechanisms, which coexist in most clinical situations, contribute to development of dysfunctional but still viable myocardium. First, "myocardial stunning" describes a state of persistent postischemic contractile dysfunction despite restoration of near-normal blood flow. In addition to "acute stunning" that occurs as a consequence of a single episode of ischemia, the definition of *myocardial stunning* has been extended to chronic left ventricular dysfunction associated with repetitive episodes of ischemia, which is then referred to as "repetitive stunning" (55). Molecular mechanisms for stunning include intracellular calcium overload caused by ischemia, which results in desensitization and lysis of myofilaments (56), and generation of oxygen-derived free radicals, which inhibit ionic pumps and mitochondrial function, at reperfusion (57).

Second, "myocardial hibernation" has been described as a consequence of reduced resting perfusion caused by severe coronary stenosis that leads to an adaptive downregulation of contractile function, which is reversible after reestablishment of normal perfusion (51,58).

**Figure 2**

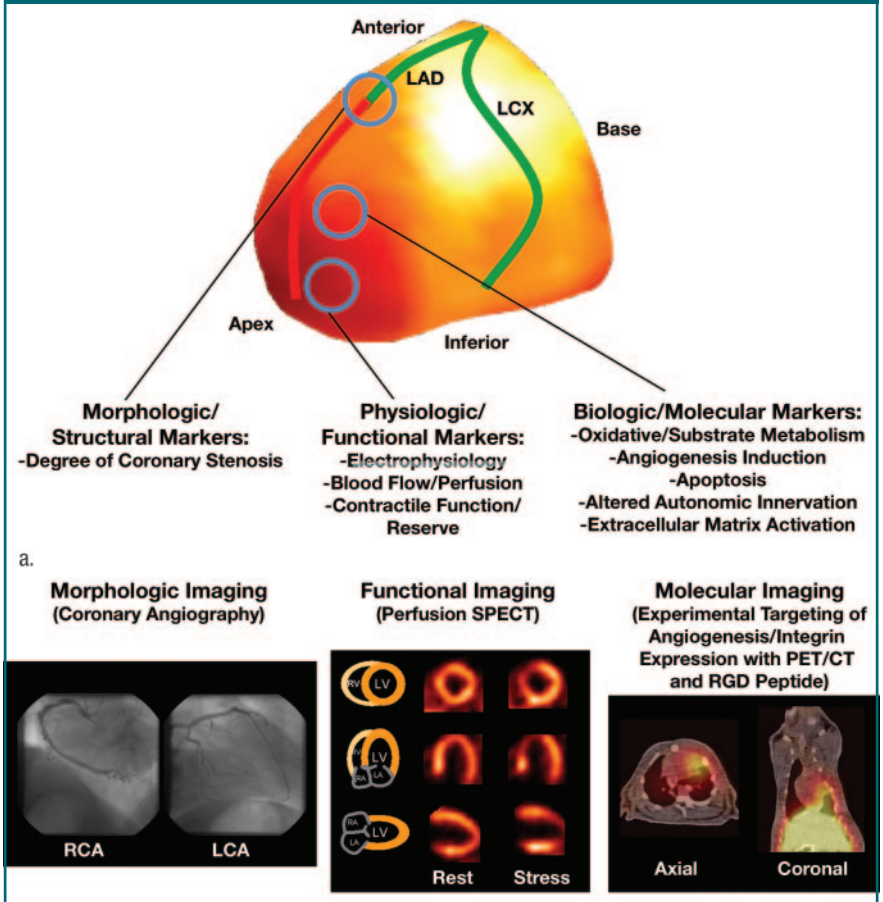


**Figure 2:** Imaging in myocardial ischemia. **(a)** Imaging markers in CAD. **(b)** Examples of morphologic, functional, and molecular images. *LAD* = left anterior descending artery, *LCA* = left coronary artery, *LCX* = left circumflex artery, *RCA* = right coronary artery.

Uncoupling of contractile work and myocardial blood flow is thought to be part of this adaptation. Since approximately 60% of oxygen consumption is linked to contractile performance, energy can be saved and the tolerance to ischemia can be increased at the expense of regional dysfunction. It has been shown that this adaptive process is associated with molecular alterations, such as dedifferentiation of myocytes, decreased expression of contractile proteins, accumulation of glycogen, loss of sarcoplasmic reticulum, small mitochondria, and increasing interstitial fibrosis (59–61).

The prediction of functional recovery by using detection of myocardial viability has emerged as a clinical application for molecular imaging. Reversible left ventricular dysfunction is generally associated with maintained or even increased tissue uptake of the glucose metabolic marker FDG (62–64). Hibernating and repetitively stunned myocardia are characterized by a perfusion-metabolism mismatch pattern with reduced regional uptake of a perfusion tracer but preserved uptake of FDG metabolic tracer. Scar tissue, on the other hand, is characterized by a matched reduction of perfusion and FDG uptake (Fig 3). Studies of myocardial metabolism by using FDG and PET have provided important information for a better understanding of the pathophysiologic interrelations among myocardial blood flow, substrate metabolism, and contractile function in ischemically compromised myocardium. These studies have also played a fundamental role in the clinical emergence of noninvasive viability imaging and are regarded as an imaging reference standard (65,66). An extensive body of literature exists that documents the diagnostic accuracy of FDG PET for prediction of functional recovery after revascularization. In addition, the prognostic value of PET has been described (67,68), and the perfusion-metabolism mismatch has been identified as an unstable state associated with a high risk and poor outcome if not treated immediately (69,70).

Other techniques have been introduced for prediction of functional recovery and were validated compared with PET metabolic imaging (71,72). Studies of the contractile response to low-dose dobutamine by using echocardiography or MR imaging were shown to be diagnostically useful. Measurements of contractile reserve have a marginally higher specificity but somewhat lower sensitivity for prediction of functional recovery when compared with FDG metabolic imaging (71). This has been explained by the fact that FDG may be used to detect residual viable tissue in some areas where extensive fibrosis already coexists. These areas of advanced hibernation may show only slow functional improvement but may still be important to revascularize because of an association with poor outcome (73).

Further, MR imaging has been used to identify scar tissue by means of the retention of gadolinium-based contrast agent. Imaging of gadolinium-based contrast agent late enhancement allows accurate detection of the regional and transmural extent of irreversibly damaged myocardium. It has been shown that the transmural extent of gadolinium-based contrast agent enhancement is correlated with the likelihood of regional functional recovery (74). The diagnostic and prognostic accuracy of this test, however, needs to be defined in detail. Findings in other studies have suggested that functional measures of regional viability may be superior to the static measurement of the extent of necrotic tissue for prediction of recovery (75) and, thus, that biologic and molecular mechanisms other than scar devel-

**Figure 3**

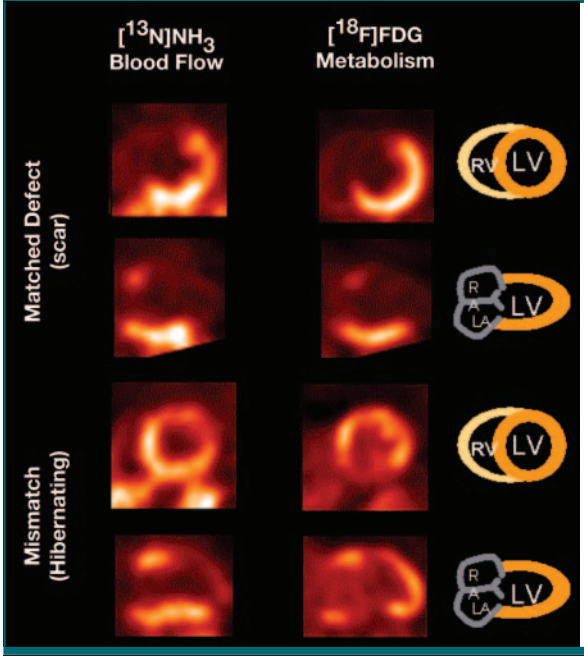


**Figure 3:** Examples of patterns of myocardial viability from perfusion-metabolism PET imaging. Representative left ventricular *(LV)* short- and long-axis sections from two patients with severe ventricular dysfunction are depicted in "hot metal" color scale (brighter color indicates higher radioactivity concentration). In top two rows, an anteroseptal perfusion defect is present in [$^{13}$N]—$NH_3$ perfusion images, with concomitant matched reduction of uptake of the metabolic tracer FDG. This pattern indicates the presence of scar tissue, which will not benefit from revascularization. In bottom two rows, a perfusion defect is shown in the anterior and apical wall. Enhanced FDG uptake is found in the metabolic study, indicating the presence of ischemically compromised hibernating myoardium, which will benefit from revascularization. Note that relatively reduced uptake of FDG in normally perfused inferior wall is consistent with use of fatty acids as substrate in this area of normally perfused myocardium. *LA* = left atrium, *RA* = right atrium, *RV* = right ventricle.

opment are important in chronic ischemic ventricular dysfunction.

Innovations in molecular imaging may allow refinement of the characterization of jeopardized myocardium and, thus, further improvement of diagnostic and prognostic assessment of myocardial viability in the future. The extent of apoptotic cell death in hibernating myocardium may be identified by using tracers such as radiolabeled annexin V. This may allow one to identify the severity of ischemic damage and the transition from programmed cell survival to programmed cell death. Other biologic targets for molecular imaging in chronic dysfunctional myocardium may be extracellular matrix activation, collagen deposition, or inflammation. Finally, multimodality imaging may be of special value in chronic left ventricular dysfunction by providing a combination of morphologic, functional, and metabolic information (Fig 4).

**Figure 4**

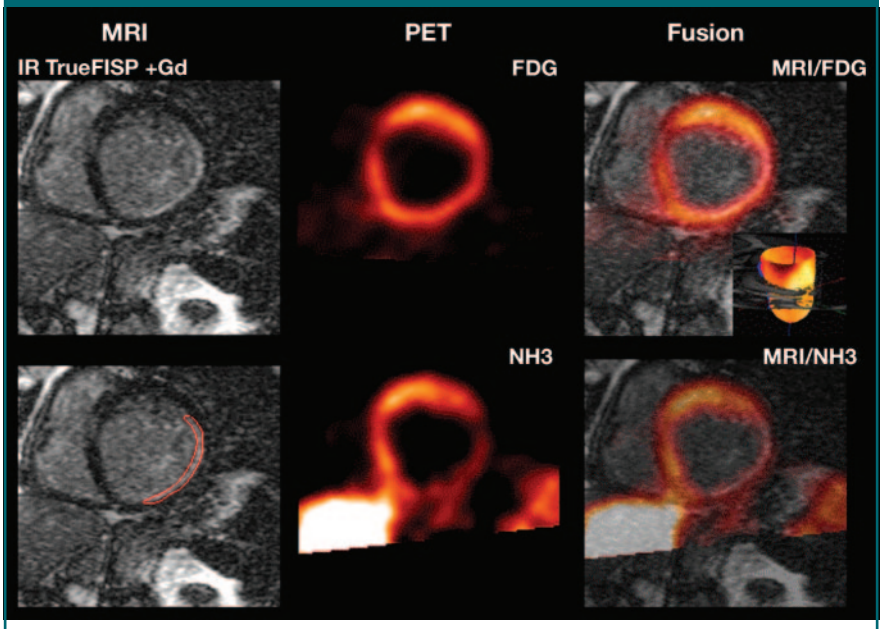


**Figure 4:** Multimodality imaging of myocardial viability. Short-axis MR images show late enhancement of gadopentetate dimeglumine (in gray scale) and PET images show glucose metabolism (using FDG) and perfusion (using [$^{13}$N]—$NH_3$*[NH3]*). PET images are displayed in a hot metal color scale where brighter color indicates higher radioactivity concentration. Nontransmural late enhancement, indicating subendocardial scar tissue, is shown on MR images. PET scans show reduced perfusion in the same area (bottom middle), but FDG uptake is less reduced and higher compared with perfusion (top middle). This perfusion-metabolism mismatch indicates residual viability in the subepicardial portion of the area with subendocardial scar. *IR TrueFISP + Gd* = inversion-recovery true fast imaging with steady-state precession and gadolinium-based contrast agent.

## Heart Failure

In the United States, approximately 5 million patients have HF, with an estimated 500 000 new cases diagnosed each year (76). HF is the leading cause of morbidity, mortality, and hospitalization in patients older than 60 years and is the most common Medicare diagnosis-related group (77). The direct and indirect cost of HF was estimated at $23.2 billion in 2002 (78). Clearly, this disease exerts major societal burden and costs. Yet, despite recent advances in medical therapy, nearly 300 000 patients will die of HF as a primary or secondary cause each year (79). Therefore, other treatment approaches, such as implantable cardioverter defibrillator (ICD), cardiac resynchronization therapy, cardiac gene therapy, and cardiac stem cell transplantation, have been advocated. The last two subjects will be discussed in subsequent sections of this article.

It is known that approximately 50% of all HF deaths are caused by ventricular tachycardia and approximately 80% of patients with symptomatic systolic dysfunction have ventricular tachycardia (80). Results of the Multicenter Automatic Defibrillator Implantation Trial (also known as MADIT-II) showed that routine implantation of ICDs in patients with a prior MI and an ejection fraction of less than 30% led to reduction of mortality rates from 19.8% (conventional therapy group) to 14.2% (ICD group) (hazard ratio = 0.69, $P$ = .16) (81). Findings in this study suggested that ICD implantation should be considered routinely in all patients with reduced ventricular ejection fraction after MI (82). Besides risk of sudden cardiac death, patients with HF can have intraventricular dyssynchrony (or left bundle branch block), which causes the two ventricles to beat in an asynchronous fashion, reduces systolic function, and increases systolic volume.

Intraventricular dyssynchrony is seen in approximately 15%–30% of patients with HF (83). Cardiac resynchronization therapy paces both the right and left ventricle, which can synchronize the activation of the heart and, thus, improve left ventricular systolic function (84). This differs from the typical pacemaker, which paces only the right ventricle. In the Multicenter InSync Randomized Clinical Evaluation (also called MIRACLE), results indicated that cardiac resynchronization therapy improved symptoms, exercise tolerance, and quality of life substantially (84). However, the estimated cost of cardiac resynchronization therapy and/or ICD and hospitalization for implantation is between $40 000 and $50 000 per patient (78). Applying this expense to the estimated 400 000 to 1.5 million patients with HF who may benefit from ICD poses an astronomic burden to health care costs. In addition, an estimated 20%–30% of patients do not respond to cardiac resynchronization therapy (85). Thus, these issues empha-

size the need for additional measures that can be used to selectively identify which patients will benefit the most from ICD and cardiac resynchronization therapy.

Traditionally, the single most useful diagnostic test for the evaluation of patients with HF is two-dimensional echocardiography coupled with a Doppler flow study. Echocardiography can provide global and regional function, degree of ventricular remodeling, contractile reserve, ischemia, and viability, particularly in patients after acute coronary syndromes or patients with chronic HF. However, these measurements do not address the issue of intraventricular conduction delays. Newer echocardiographic measurements, which include tissue Doppler imaging (86), strain rate imaging (87), and tissue tracking (88), have all been advocated. These parameters may provide optimal information on intraventricular dyssynchrony and allow prospective identification of responders to cardiac resynchronization therapy (89). A detailed discussion of each modality is beyond the scope of this review, but interested readers should refer to published articles (89,90).

Investigators in several studies have also demonstrated that $^{123}$I-MIBG imaging can provide powerful diagnostic and prognostic information in patients with HF. Many radiotracers for scintigraphic imaging of cardiac neurotransmission have been developed with radiolabeling of the neurotransmitters or their structural analogs (Fig 5a). Of these, MIBG shares many cellular uptake and storage properties with norepinephrine, and, thus, MIBG scans have been used to evaluate cardiac sympathetic nervous system distribution and function. In patients with HF, MIBG scans typically show a reduced heart-mediastinum uptake ratio, heterogeneous distribution within the myocardium, and increased MIBG washout from the heart (91–93) (Fig 5b, 5c). For example, Arimoto et al (94) showed that patients with abnormally rapid washout levels had a significantly higher cardiac event rate than did those with normal washout levels (57% vs 12%, $P < .0001$) during the follow-up period (6–30 months).

Kyuma et al (95) showed incremen-

**Figure 5**

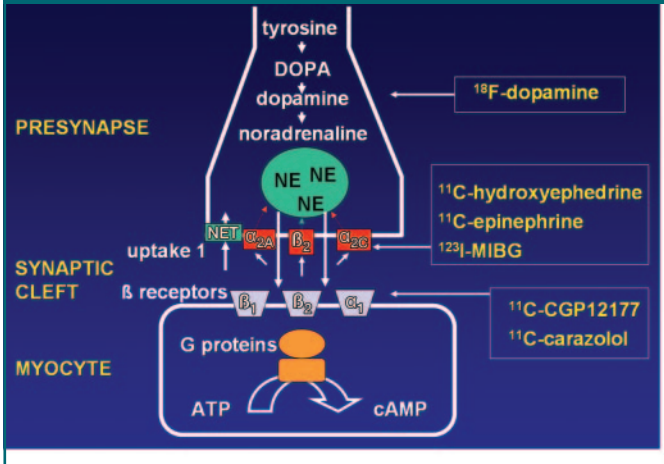


a.

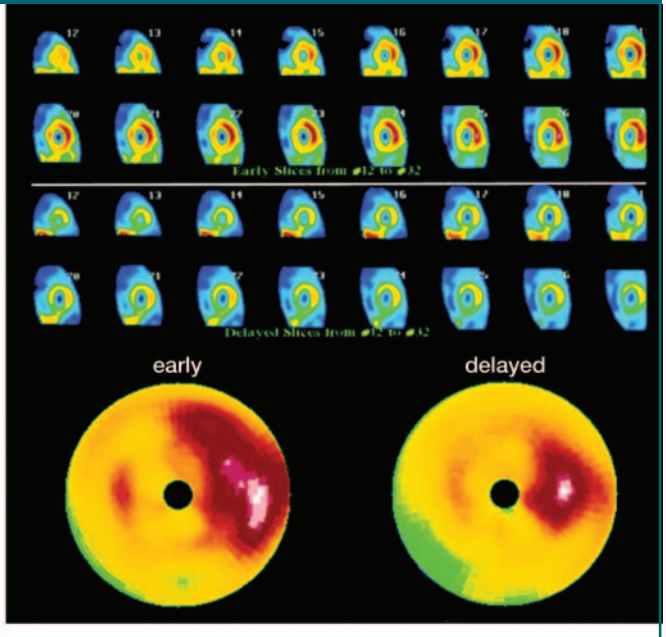


b.

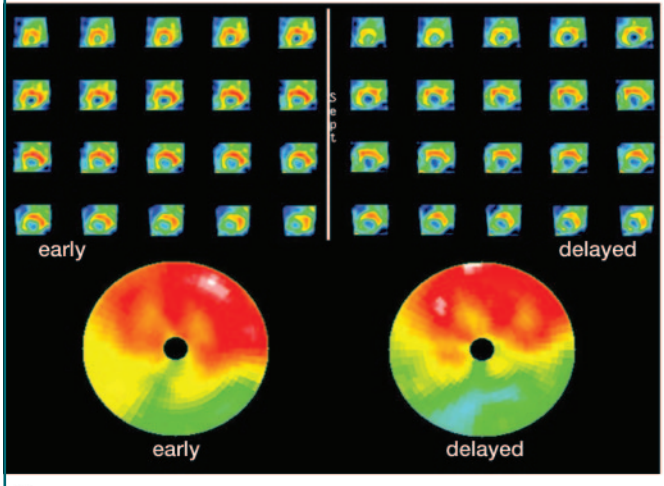


c.

**Figure 5:** $^{123}$I-MIBG imaging in patients with HF. **(a)** Schematic shows most commonly used radioligands for assessment of cardiac pre- and postsynaptic processes. **(b)** SPECT MIBG study in healthy volunteer. Short-axis tomograms and reconstructed polar maps show normal MIBG distribution and washout. **(c)** SPECT MIBG study in patient with dilated cardiomyopathy. Short-axis tomograms and reconstructed polar maps show decreased and heterogeneous myocardial MIBG activity. *ATP* = adenosine triphosphate, *DOPA* = dihydroxyphenylalanine, *cAMP* = cyclic adenosine monophosphate, *NE* = norepinephrine. (Reprinted, with permission, from reference 91.)

tal prognostic levels when the plasma brain natriuretic peptide level and the heart-mediastinum uptake ratio were used together. More important, in a pilot study, Arora et al (96) showed that patients with ICD discharge had a substantially lower MIBG heart-mediastinum tracer uptake ratio, higher MIBG defect scores, and more extensive sympathetic denervation. Clearly, larger studies are needed in the future. If confirmed, cardiac autonomic assessment by using MIBG scans may help in the selection of patients who would benefit the most from an ICD by means of identification of those at increased risk for potentially fatal arrhythmias, leading to more cost-effective implementation of this life-saving device.

## Cardiac Gene Therapy

Gene transfer has been heralded as the most promising therapy of molecular medicine in the 21st century. It is usually defined as the transfer and expression of DNA to somatic cells in an individual, with a resulting therapeutic effect. In cardiovascular diseases, gene therapy offers an exciting new approach to express the therapeutic factors locally in the myocardium (97). In general, the successful application of gene therapy requires three essential elements: *(a)* a vector for gene delivery, *(b)* delivery of the vector to the target tissue, and *(c)* a therapeutic gene to be expressed in a particular patient population.

An ideal vector should enable efficient gene delivery to the target tissue, have minimal local or systemic toxicity, deliver enough concentration and duration to induce a therapeutic effect, and cause no germ-line transmission to the offspring. No single vector has all of these attributes, and, therefore, the type of vector chosen will need to be tailored to the specific clinical applications. Vectors can be classified as viral vectors and nonviral vectors. Common viral vectors include adenovirus, adeno-associated virus, gutless adenovirus, and lentivirus. Nonviral vectors include plasmids, naked DNA, and liposomes (98). The technique of vector delivery to the heart also depends on the intended target area but in general can be categorized as the following: *(a)* direct epicardial injection, *(b)* endocardial injection, *(c)* intracoronary infusion, *(d)* retrograde coronary sinus infusion, and *(e)* pericardial injection (99).

Likewise, the choice of a therapeutic gene to be expressed is often driven by the intended application. In animal studies, successful gene therapy has been demonstrated for the following: *(a)* the treatment of CAD by using angiogenic factors such as vascular endothelial growth factor (VEGF) (100), fibroblast growth factor (101), and hypoxia-inducible factor 1α (102); *(b)* reduction of restenosis after angioplasty through inhibition of smooth muscle cell proliferation with suicide gene therapy by using thymidine kinase (103); *(c)* improvement of congestive HF with gene transfer of a calcium adenosine triphosphatase pump (*SERCA2a*) (104); *(d)* inhibition of atherosclerosis with overexpression of an high-density lipoprotein receptor (105); and *(e)* reduction of hypoxia-induced apoptosis of cardiomyocytes (106).

These encouraging results led to the initiation of several clinical trials beginning in the 1990s. Of the 509 ongoing gene therapy trials in the United States, 46 are related to cardiovascular diseases (107). The majority of these studies are aimed at testing the safety and efficacy of therapeutic angiogenesis and, to a lesser extent, examining restenosis. In the late 1990s, results of several phase 1 open-labeled trials that involved small numbers of patients with myocardial ischemia and peripheral vascular disease were uniformly positive (108–110). However, phase 2 randomized, double-blind, placebo-controlled trials have yielded conflicting, if not disappointing, results. In the Vascular Endothelial Growth Factor in Ischemia for Vascular Angiogenesis (also known as VIVA) (111), FGF Initiating Revascularization Trial (also called FIRST) (112), Adenovirus Fibroblast Growth Factor Angiogenic Gene Therapy (also known as AGENT) (113,114), and the Kuopio Angiogenesis Trial (also called KAT) (115), gene therapy was tested by using either vascular endothelial growth factor (VEGF) or fibroblast growth factor. Unfortunately, these trials failed to show any consistent improvement in various parameters, such as symptoms, ejection fraction, wall motion scores, myocardial perfusion, and restenosis rate.

Nonetheless, important lessons can be learned from these trials. They showed that angiogenesis is a complex process regulated by the interaction of various growth factors and may be difficult to stimulate by using a single protein or gene injection. The ideal injection method, delivery vector, and patient population remain to be determined. The pharmacokinetics and pharmacodynamics of therapeutic gene expression will need to be defined first before gene therapy can proceed further to widespread clinical use, and this process is similar to that for the research and development of experimental drugs. Finally, since there is no available method of assessing gene expression in vivo, investigators are unable to determine whether the lack of symptomatic improvement is due to poor injection technique, insufficient gene expression, the host inflammatory response, or an inappropriate therapeutic gene (116).

Most molecular imaging studies have focused on cancer biology (117, 118). Imaging of cardiac transgene expression was established in several proof-of-principle studies that involved the injection of various reporter genes into the myocardium and in which the kinetics of transgene expression was followed over time by using optical bioluminescence, micro-PET, and clinical PET imaging (119–123). The concept of imaging reporter gene expression (Fig 6) involves a reporter gene first being introduced into target tissues by various methods, which include viral and nonviral vectors. The upstream promoter that regulates the transcription of the reporter gene can be constitutive (always on), inducible (can be turned on or off), or tissue specific (expressed only in the tissues of interest).

Transcription of the reporter gene and translation of the messenger RNA lead to a reporter protein product that can interact with the reporter probe. This interaction may be enzyme based (eg, phosphorylation of a reporter probe with intracellular retention of metabolites) or receptor based (eg, binding of a radiolabeled ligand to cell surface receptors) (98). Clearly, much flexibility exists within these systems. By altering various components, the reporter gene can provide information about the efficiency of vector transfection into cells, regulation of DNA by upstream promoters, and the fate of intracellular protein trafficking. In addition, the reporter probe itself does not

**Figure 6**

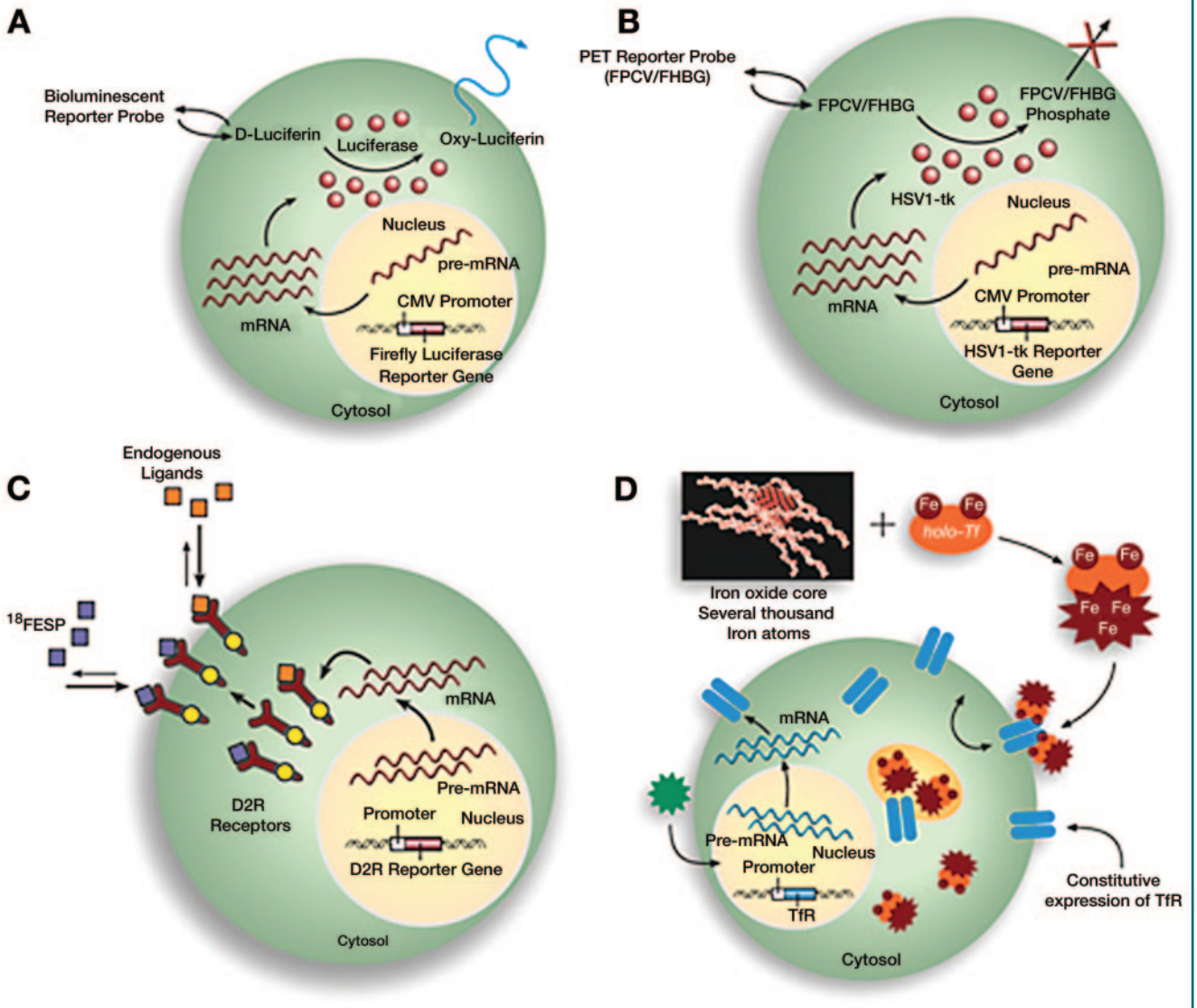


**Figure 6:** Four strategies of imaging reporter gene and reporter probe. *A,* Enzyme-based bioluminescence imaging. Expression of the firefly luciferase reporter gene leads to the firefly luciferase reporter enzyme, which catalyzes the reporter probe (D-luciferin) that results in a photochemical reaction. This yields low levels of photons that can be detected and quantified by a charge-coupled device camera. *B,* Enzyme-based PET imaging. Expression of the herpes simplex virus type 1 thymidine kinase (*HSV1-tk*) reporter gene leads to the thymidine kinase reporter enzyme, HSV1-TK, which phosphorylates and traps the PET reporter probe 9-(4-[18F]fluoro-3-hydroxymethylbutyl)guanine (FHBG) intracellularly. Radioactive decay of $^{18}$F isotopes can be detected with PET. *C,* Receptor-based PET imaging. 3-(2-[18F]fluoroethyl)-spiperone *($^{18}$FESP)* is a reporter probe that interacts with the dopamine 2 receptor *(D2R)* to result in probe trapping on or in cells expressing the *D2R* gene. *D,* Receptor-based MR imaging. Overexpression of engineered transferrin receptor *(TfR)* results in increased cell uptake of the transferrin-monocrystalline iron oxide nanoparticles. These changes result in a detectable contrast change on MR image. *FPCV* = 8-[18F]fluoropenciclovir, *holo-Tf* = holo-transferrin. (Reprinted, with permission, from reference 98.)

have to be changed if one wishes to study a new biological process, which saves valuable time needed to synthesize, test, and validate new radiotracer agents.

The feasibility of linking a PET reporter gene to a therapeutic gene was demonstrated in two separate studies (124,125). In this case, an adenovirus containing two constitutive cytomegalovirus (CMV) promoters driving a $VEGF_{121}$ therapeutic gene and an *HSV1-sr39tk* PET reporter gene separated by poly-adenine sequences was constructed (Ad-CMV-$VEGF_{121}$-CMV-HSV1-sr39tk) (Fig 7a). Wu et al injected the construct into the myocardium of a rat in an MI model. Reporter gene expression, which indirectly reflects the $VEGF_{121}$ therapeutic gene expression, persisted for only approximately 2 weeks because of host immune response against the adenovirus (124). At 2 months, there was no substantial improvement in myocardial contractility, perfusion, or metabolism as measured by using echocardiography, $^{13}N$ ammonia ($[^{13}N]$—$NH_3$) perfusion, and FDG imaging between study and control groups (Fig 7b). Thus, this study highlights the importance of monitoring the pharmacokinetics of gene expression. It also demonstrates the proof of principle that any other cardiac therapeutic genes of interest (eg, hypoxia-inducible factor 1α, sarcoplasmic endoplasmic reticulum $Ca^{2+}$, heat shock protein, or endothelial nitric oxide synthase) can likewise be coupled to a PET reporter gene for subsequent noninvasive monitoring.

In the future, it will also be useful to have the following arsenals for cardiac gene therapy: *(a)* less immunogenic vectors such as adenoassociated virus that can prolong transgene expression in the myocardium (126); *(b)* cardiac tissue-specific promoter (eg, myosin light chain kinase or troponin) that can diminish unwanted extracardiac activity (82); *(c)* codelivery of proangiogenic genes with stem cells to enhance revascularization (127); and *(d)* multimodality molecular imaging approaches that can monitor the location, magnitude, and duration of transgene expressions, as well as their downstream functional effects (98,116).

**Figure 7**

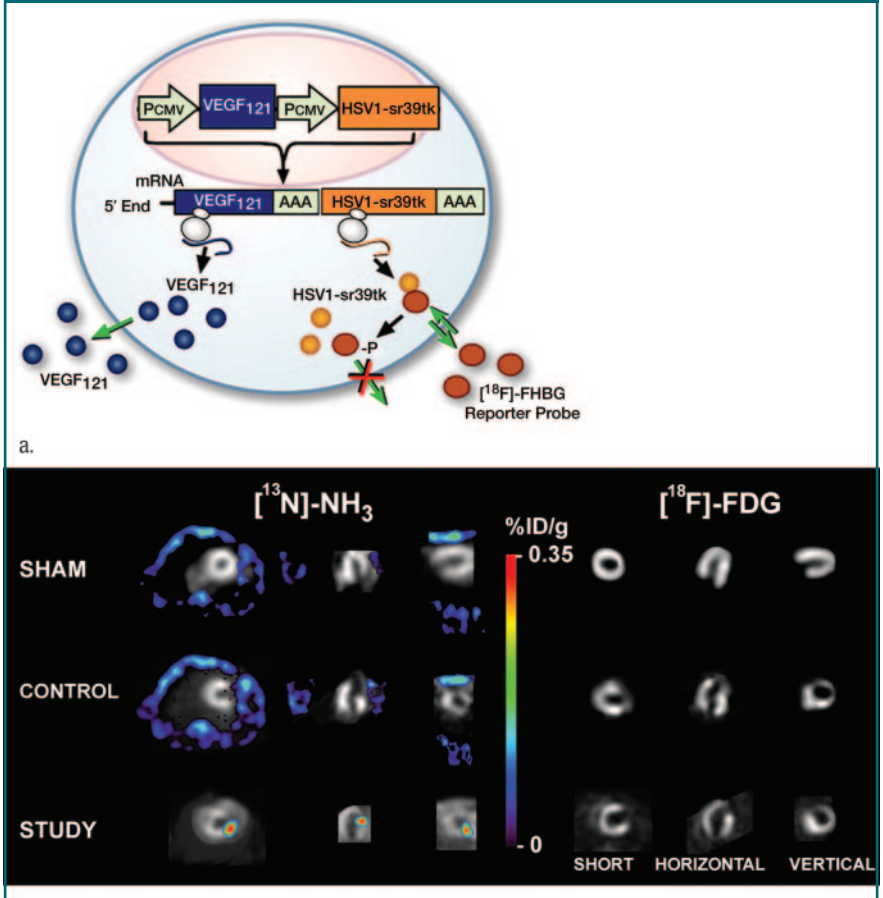


**Figure 7:** Molecular imaging of cardiac perfusion, metabolism, and gene expression. **(a)** Schematic of Ad-CMV-$VEGF_{121}$-CMV-HSV1-sr39tk mediated gene expression. The translated product of $VEGF_{121}$ is soluble and excreted extracellularly, whereas the translated product of *HSV1-sr39tk* (HSV1-sr39TK) traps FHBG intracellularly by phosphorylation. $P_{CMV}$ = CMV promoter. **(b)** At day 2, representative images showing normal perfusion ($[^{13}N]$—$NH_3$) and metabolism (FDG) in a sham rat, anterolateral infarction in a control rat, and anterolateral infarction in a study rat (Ad-CMV-$VEGF_{121}$-CMV-HSV1-sr39tk) in short, vertical, and horizontal axis (gray scale). The color scale is expressed as percentage injected dose per gram *(%ID/g)* for FHBG uptake. Only the study rat showed robust *HSV1-sr39tk* reporter gene activity near the site of injection. (Reprinted, with permission, from reference 124.)

## Stem Cell Transplantation

In an acute MI, tissue loss leads to hemodynamic stress followed by compensatory left ventricular hypertrophy and dilatation. Many patients continue to develop refractory HF symptoms and require more aggressive approaches, such as a left ventricular assist device and orthotopic heart transplantation. However, the limitations of these approaches (eg, infection and bleeding for left ventricular assist device and organ shortage and graft rejection for orthotopic heart transplantation) justify the search for alternative therapeutic options.

Stem cell transplantation holds potential promise for treatment of ischemic heart disease. Orlic et al (128) reported transdifferentiation of bone marrow–derived hematopoietic stem cells into cardiomyocytes after myocardial

**Figure 8**

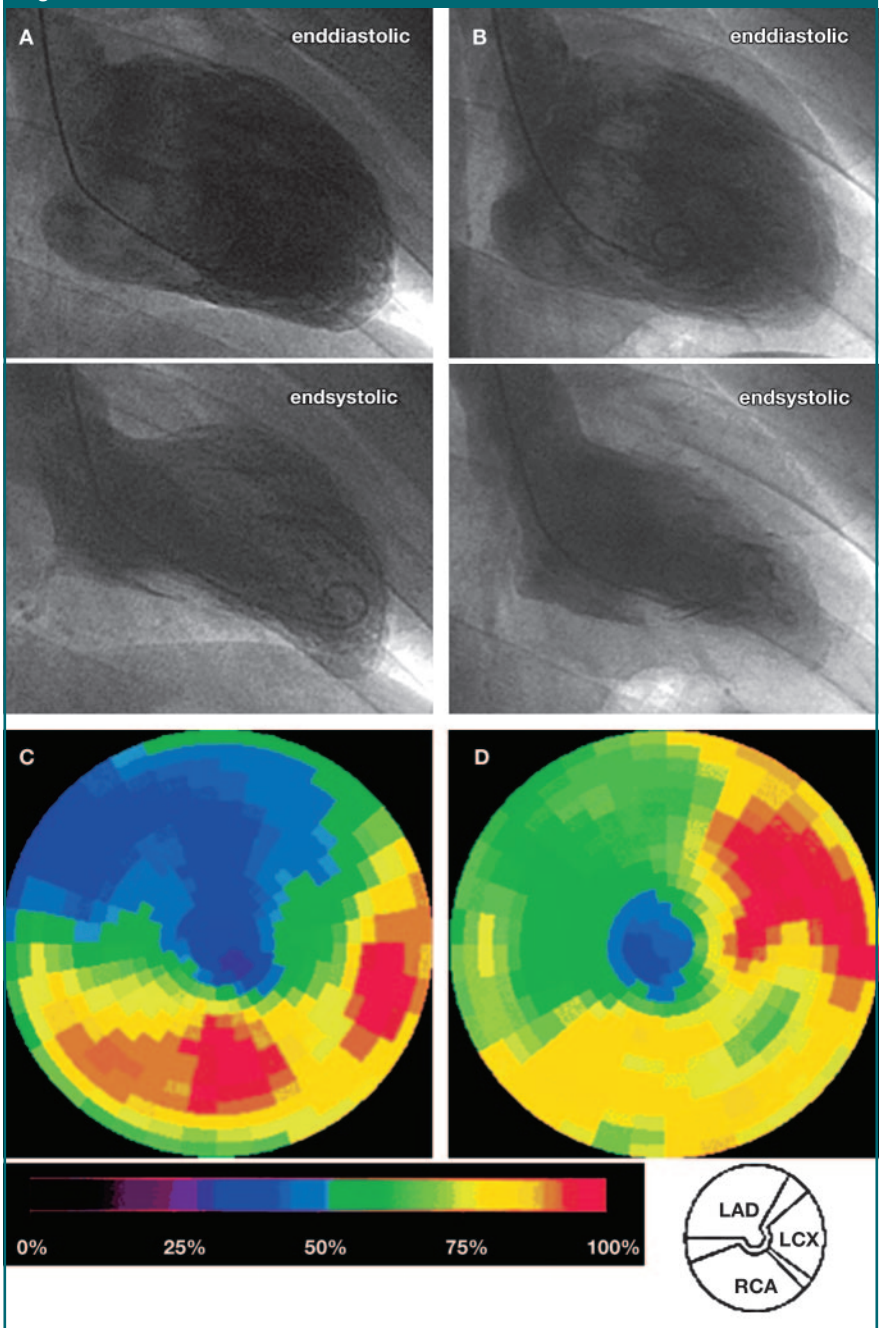


**Figure 8:** Functional imaging studies in a patient after MI who underwent intracoronary infusion of circulating blood–derived progenitor cells. *A,* Left ventricular angiograms before circulating blood–derived progenitor cell therapy and, *B,* at 4-month follow-up. *C,* Pretherapeutic and, *D,* posttherapeutic corresponding FDG PET bull's-eye views of the left ventricle of the patient. *LAD* = left anterior descending artery, *LCX* = left circumflex artery, *RCA* = right coronary artery. (Reprinted, with permission, from reference 132.)

injury in mice. However, researchers in subsequent studies have questioned the concept of differentiation across tissue lineage boundaries (129,130). Regardless, several phase 1 clinical trials involving transplantation of bone marrow stem cells, skeletal myoblasts, and endothelial progenitor cells have been initiated since then (131–138). Assmus et al (132) showed that transplantation of progenitor cells was associated with a substantial increase in global left ventricular ejection fraction, improved regional wall motion in the infarct zone, and reduced end-systolic left ventricular volumes at 4-month follow-up (Fig 8).

Wollert et al (138) showed that the mean global left ventricular ejection fraction, as determined with cardiac MR imaging, increased by 6.7% in patients after MI who received autologous bone marrow stem cells ($n = 30$) compared with 0.7% in the control group ($n = 30$) ($P = .0026$). The mechanisms of improvement may be related to improved angiogenesis or vasculogenesis, better survival of hibernating myocardium, paracrine effects of injured cells, or modulation of the wound tissue. Interestingly, the 18-month follow-up data from the same study showed that the difference in left ventricular ejection fraction was no longer significant ($P = .27$) (139). The authors suggested that bone marrow stem cell transplantation may not lead to substantial formation of new myocardial tissues and that pharmacologic or genetic strategies may be warranted to enhance myocardial engraftment and increase its therapeutic efficacy.

One of the main limitations of cardiac stem cell transplantation is the lack of available methods to assess stem cell survival. In clinical studies, changes in myocardial perfusion, viability, and perfusion are assessed with echocardiography, nuclear SPECT and PET imaging, or MR imaging (Table 2). These parameters can be used to measure the therapeutic effects but not to actually detect the presence or absence of transplanted stem cells. This is an important distinction because most patients also undergo concurrent coronary artery bypass graft or percutaneous coronary in-

**Table 2**

**Phase 1 Clinical Trials of Stem Cell Therapy**

| Study and Year | No. of Patients | Delivery Method | Follow-up | Cell Type | Results | Imaging Modalities |
|---|---|---|---|---|---|---|
| Strauer et al (131), 2002 | 10 | Percutaneous coronary intervention | 3 mo | Bone marrow stem cells | Increased perfusion and contractility | $^{201}$Tl SPECT, dobutamine stress echocardiography, left ventricular angiography |
| Assmus et al (132), 2002 | 20 | Percutaneous coronary intervention | 4 mo | Endothelial progenitor cells | Increased perfusion and contractility | FDG PET, dobutamine stress echocardiography, left ventricular angiography |
| Menasche et al (133), 2003 | 10 | Coronary artery bypass graft | 10.9 mo | Skeletal myoblasts | Improved contractility and HF symptoms | FDG PET, dobutamine stress echocardiography |
| Pagani et al (134), 2003 | 5 | Left ventricular assist device | 68–191 d | Skeletal myoblasts | Development of mature myofiber seen at immunohistochemical analysis | . . . |
| Tse et al (135), 2003 | 8 | Electromechanical mapping with percutaneous catheter | 3 mo | Bone marrow stem cells | Improved perfusion, contractility, and anginal symptoms | MR imaging |
| Perin et al (136), 2003 | 14 | Electromechanical mapping with percutaneous catheter | 4 mo | Bone marrow stem cells | Improved perfusion and contractility | Techetium 99m sestamibi SPECT, two-dimensional echocardiography, left ventricular angiography |
| Stamm et al (137), 2004 | 12 | Coronary artery bypass graft | 3–9 mo | Bone marrow stem cells | Improved perfusion | $^{201}$Tl SPECT |
| Wollert et al (138), 2004 | 30 | Percutaneous coronary intervention | 6 mo | Bone marrow stem cells | Improved contractile function | MR imaging |

Note.—$^{201}$Tl = thallium 201.

tervention, and it is not clear whether the improvement is due to these procedures or to the transplanted stem cells. Likewise, in animal studies, analysis of stem cell survival is based on postmortem histologic examination, which is invasive and precludes longitudinal monitoring (128–130,140). Thus, the ability to study stem cells in the context of the intact whole-body system rather than with indirect (clinical trials) or invasive (animal studies) means will give better insight into the underlying biology and physiology of stem cells. Several investigators have started addressing this issue through different approaches, including radionuclide labeling, ferromagnetic labeling, and reporter gene labeling (Table 3).

For radionuclide labeling, Aicher et al (141) injected endothelial progenitor cells with indium 111 ($^{111}$In) oxine into nude rats with infarcted myocardium. At 24 to 96 hours, images obtained with a double-headed gamma camera showed that the ratio of specific radioactivity of the heart was approximately twice the activity of peripheral skeletal muscle tissue. The main limitation of this approach is that $^{111}$In-oxine has a physical half-life of 2.8 days, so cell distribution can be studied only for 5–7 days. For ferromagnetic labeling, Kraitchman et al (142) injected swine mesenchymal stem cells with ferumoxides injectable solution (Feridex; Berlex, Montville, NJ), with 25 μg of iron per milliliter, into pig hearts. Images were obtained by using a 1.5-T MR imager (CV/i; GE Medical Systems, Milwaukee, Wis). After 24 hours, the injected sites appeared as ovoid hypointense lesions with sharp borders. At 1–3 weeks after cell injection, the delineation of the borders was less clear because of degradation of the ferumoxides particles. The main limitation of MR imaging for this application is its lack of capability for use in a serial fashion. Because ferumoxides injectable solution will still register an MR signal even when the injected cells have undergone apoptosis or cell death, it may be difficult to relate the MR signal to the number of viable cells.

For reporter gene labeling, the cells are transfected with reporter genes

prior to implantation into the myocardium. If the cells are alive, the reporter gene will be expressed. If the cells are dead, the reporter gene will not be expressed. By using this approach, Wu et al (143) injected embryonic cardiomyoblasts expressing either firefly luciferase or *HSV1-sr39tk* reporter genes that were tracked noninvasively by using optical bioluminescence or micro-PET imaging, respectively (Fig 9). Drastic reductions of signal intensity within the first 1–4 days were noted and were likely due to acute donor cell death from inflammation, adenoviral toxicity, ischemia, and apoptosis. The pattern of cell death was consistent with data in other reports in which invasive assays, such as serial histologic staining (144), terminal transferase uridyl nick end labeling apoptosis assays (145), and TaqMan real-time polymerase chain reaction assays, were used (146).

In contrast, transplantation of mouse embryonic stem cells in the myocardium led to intracardiac and extracardiac teratoma formation, as determined by using molecular imaging techniques, and raised serious doubts about the use of undifferentiated embryonic stem cells for myocardial regeneration (147). Interestingly, the PET reporter gene (herpes simplex virus type 1 truncated thymidine kinase [*HSV1-ttk*]) can also serve as a suicide gene by treating the animals with ganciclovir and allows for a backup safety measure against stem cell misbehavior. Finally, the safety of reporter gene expression in stem cells was recently evaluated by comparing the transcriptional profile of normal mouse embryonic stem cells versus embryonic stem cells stably expressing fluorescence (monomeric red fluorescence protein), bioluminescence (firefly luciferase), and PET (*HSV1-ttk*) fusion reporter genes (148). Of 20 371 genes analyzed, there were only 296 genes, representing approximately 1.4% of total genes, that had more than twofold up- or downregulation on the basis of gene ontology annotation. More important, expression of these reporter genes had no major adverse effects on embryonic stem cell viability, proliferation, or differentiation.

In the future, it will be important to use these molecular imaging approaches to assess the in vivo biology of different stem cell types. Because of its noninvasive nature, molecular imaging has the potential to help accelerate research progress through evaluation of variables such as the optimal cell type, cell dosage, or delivery route. Perhaps even more important is the investigation of the means aimed at preventing acute donor cell death, which may be the most critical variable for determining the efficacy of stem cell therapy (149–151). Ultimately, the goal is to develop and standardize stem cell transplantation protocols that are safe, quantifiable, and reproducible in the future, thereby avoiding the controversies that have plagued cardiac gene therapy trials (152).

## Conclusion

In summary, molecular imaging is an exciting field. It combines the disciplines of molecular biology, radiochemistry, pharmacology, instrumentation, and clinical medicine into a new imaging paradigm. As discussed in this review, molecular imaging can be used to study cardiac neurotransmission, plaque vulnerability, inflammation, myocardial viability, as well as newer research sub-

**Table 3**

**Imaging Strategies in Cardiovascular Diseases**

| Target | Past Strategy | Present Strategy | Future Strategy |
|---|---|---|---|
| Atherosclerosis | Invasive angiography | Invasive angiography and intravascular US, CT angiography | Invasive angiography and optical coherence tomography; noninvasive angiography with CT and MR imaging; morphologic and biologic plaque characterization with CT, MR imaging, and nuclear imaging |
| Ischemia | Perfusion SPECT, stress echocardiography | SPECT, PET, echocardiography, and MR imaging of perfusion and function | One-stop shop MR imaging of morphology, function, perfusion, and viability; hybrid SPECT/CT and PET/CT imaging; molecular imaging with markers of ischemic memory, remodeling, and myocardial adaptive mechanisms |
| Viability | FDG PET, $^{201}$Tl SPECT | FDG PET, dobutamine echocardiography, and gadolinium-enhanced MR imaging | One-stop shop MR imaging of morphology, function, perfusion, and viability; multimodality imaging of biology, contractile reserve, and geometry |
| HF | Two-dimensional and Doppler echocardiography | Two-dimensional and Doppler echocardiography | Echocardiography with tissue Doppler imaging, strain rate imaging, and tissue tracking to help select candidates for cardiac resynchronization therapy; nuclear imaging with $^{123}$I-MIBG to help select candidates for ICD implantation |
| Gene therapy | None | Functional imaging with SPECT, PET, and echocardiography | Functional imaging and molecular imaging of cardiac transgene expression |
| Stem cell therapy | None | Functional imaging with SPECT, PET, echocardiography, and MR imaging | Functional imaging and molecular imaging of stem cell survival and proliferation |

**Figure 9**

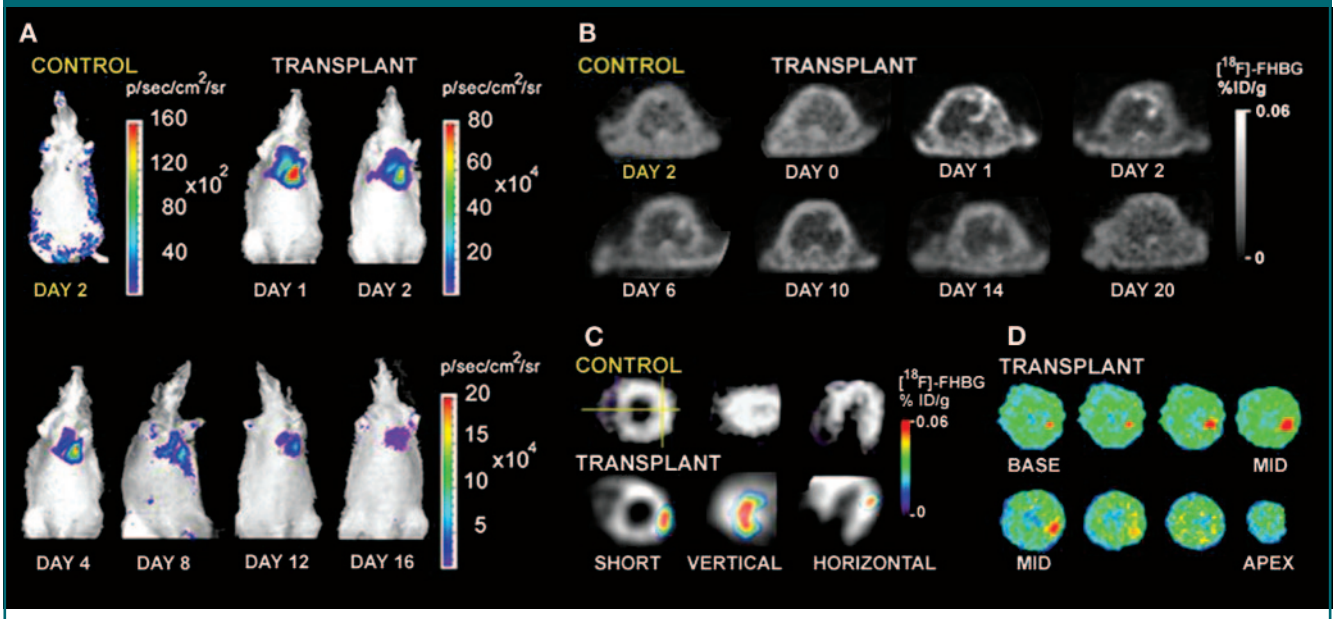


**Figure 9:** Optical bioluminescence and PET imaging of cell transplantation in rat myocardium. *A,* Study animal transplanted with embryonic H9c2 cardiomyoblasts emits significant cardiac bioluminescence activity at days 1, 2, 4, 8, 12, and 16 ($P < .05$ vs control). Control rat shows background signal only. *B,* The location, magnitude, and duration of cell survival are determined by longitudinal imaging of FHBG activity (gray scale) within the same rat. *C,* Tomographic views of cardiac micro-PET images shown in short, vertical, and horizontal axes. At day 2, study animal transplanted with cardiomyoblasts expressing *HSV1-sr39tk* shows significant FHBG uptake (color scale) superimposed on [$^{13}$N]—$NH_3$ images (gray scale). Control animal shows homogeneous [$^{13}$N]—$NH_3$ perfusion but background FHBG uptake. *D,* Autoradiography in the same study animal at day 2 confirms trapping of $^{18}$F by transplanted cells at the lateral wall at finer spatial resolution (approximately 50 μm). *%ID/g* = percentage infective dose per gram, *p/sec/cm2/sr* = photons per second per square centimeter per steradian. (Reprinted, with permission, from reference 143.)

jects, such as gene transfer and stem cell survival, that have generated much attention over recent years. Future directions include understanding the molecular mechanisms of individual disease processes, developing newer and more physiologic tracers that target specific disease sites, and implementing multimodality imaging approaches that produce fast throughput analysis in animal studies (optical), high-resolution images (echocardiography, MR imaging), and functional information (SPECT, PET). All of these measures will be essential as the field moves forward from translational animal studies to the clinical arena.

## References


1. Phelps ME. Inaugural article: positron emission tomography provides molecular imaging of biological processes. Proc Natl Acad Sci U S A 2000;97:9226–9233.
2. Massoud TF, Gambhir SS. Molecular imaging in living subjects: seeing fundamental biological processes in a new light. Genes Dev 2003;17:545–580.
3. Jaffer FA, Weissleder R. Seeing within: molecular imaging of the cardiovascular system. Circ Res 2004;94:433–445.
4. Davignon J, Ganz P. Role of endothelial dysfunction in atherosclerosis. Circulation 2004;109(23 suppl 1):III27–III32.
5. Naghavi M, Libby P, Falk E, et al. From vulnerable plaque to vulnerable patient:a call for new definitions and risk assessment strategies. I. Circulation 2003;108:1664–1672.
6. Achenbach S, Ropers D, Regenfus M, et al. Noninvasive coronary angiography by magnetic resonance imaging, electron-beam computed tomography, and multislice computed tomography. Am J Cardiol 2001;88:70E–73E.
7. Myerburg RJ, Interian A Jr, Mitrani RM, Kessler KM, Castellanos A. Frequency of sudden cardiac death and profiles of risk. Am J Cardiol 1997;80:10F–19F.
8. Fuster V, Badimon L, Badimon JJ, Chesebro JH. The pathogenesis of coronary artery disease and the acute coronary syndromes (1). N Engl J Med 1992;326:242–250.
9. Glagov S, Weisenberg E, Zarins CK, Stankunavicius R, Kolettis GJ. Compensatory enlargement of human atherosclerotic coronary arteries. N Engl J Med 1987;316:1371–1375.
10. Nissen SE. Clinical images from intravascular ultrasound: coronary disease, plaque rupture, and intervention—the inside view. Am J Cardiol 2001;88:16K–18K.
11. Tearney GJ, Yabushita H, Houser SL, et al. Quantification of macrophage content in atherosclerotic plaques by optical coherence tomography. Circulation 2003;107:113–119.
12. Hatsukami TS, Ross R, Polissar NL, Yuan C. Visualization of fibrous cap thickness and rupture in human atherosclerotic carotid plaque in vivo with high-resolution magnetic resonance imaging. Circulation 2000;102:959–964.
13. Becker CR, Nikolaou K, Muders M, et al. Ex vivo coronary atherosclerotic plaque characterization with multi-detector-row CT. Eur Radiol 2003;13:2094–2098.
14. Naghavi M, Madjid M, Gul K, et al. Thermography basket catheter: in vivo measurement of the temperature of atherosclerotic plaques for detection of vulnerable plaques. Catheter Cardiovasc Interv 2003;59:52–59.
15. Rudd JH, Warburton EA, Fryer TD, et al. Imaging atherosclerotic plaque inflamma-

tion with [18F]-fluorodeoxyglucose positron emission tomography. Circulation 2002;105: 2708–2711.

16. Litovsky S, Madjid M, Zarrabi A, Casscells SW, Willerson JT, Naghavi M. Superparamagnetic iron oxide-based method for quantifying recruitment of monocytes to mouse atherosclerotic lesions in vivo: enhancement by tissue necrosis factor-alpha, interleukin-1beta, and interferon-gamma. Circulation 2003;107:1545–1549.
17. Ohtsuki K, Hayase M, Akashi K, Kopiwoda S, Strauss HW. Detection of monocyte chemoattractant protein-1 receptor expression in experimental atherosclerotic lesions: an autoradiographic study. Circulation 2001; 104:203–208.
18. Narula J, Petrov A, Bianchi C, et al. Noninvasive localization of experimental atherosclerotic lesions with mouse/human chimeric Z2D3 F(ab′)2 specific for the proliferating smooth muscle cells of human atheroma: imaging with conventional and negative charge-modified antibody fragments. Circulation 1995;92:474–484.
19. Schafers M, Riemann B, Kopka K, et al. Scintigraphic imaging of matrix metalloproteinase activity in the arterial wall in vivo. Circulation 2004;109:2554–2559.
20. Kietselaer BL, Reutelingsperger CP, Heidendal GA, et al. Noninvasive detection of plaque instability with use of radiolabeled annexin A5 in patients with carotid-artery atherosclerosis. N Engl J Med 2004;350: 1472–1473.
21. Kolodgie FD, Petrov A, Virmani R, et al. Targeting of apoptotic macrophages and experimental atheroma with radiolabeled annexin V: a technique with potential for noninvasive imaging of vulnerable plaque. Circulation 2003;108:3134–3139.
22. Tsimikas S, Palinski W, Halpern SE, Yeung DW, Curtiss LK, Witztum JL. Radiolabeled MDA2, an oxidation-specific, monoclonal antibody, identifies native atherosclerotic lesions in vivo. J Nucl Cardiol 1999;6:41–53.
23. Sadeghi MM, Krassilnikova S, Zhang J, et al. Detection of injury-induced vascular remodeling by targeting activated alphavbeta3 integrin in vivo. Circulation 2004;110:84–90.
24. Iskander S, Iskandrian AE. Risk assessment using single-photon emission computed tomographic technetium-99m sestamibi imaging. J Am Coll Cardiol 1998;32:57–62.
25. Hachamovitch R, Berman DS, Shaw LJ, et al. Incremental prognostic value of myocardial perfusion single photon emission computed tomography for the prediction of cardiac death: differential stratification for risk of cardiac death and myocardial infarction. Circulation 1998;97:535–543.
26. Hachamovitch R, Berman DS, Kiat H, Cohen I, Friedman JD, Shaw LJ. Value of stress myocardial perfusion single photon emission computed tomography in patients with normal resting electrocardiograms: an evaluation of incremental prognostic value and cost-effectiveness. Circulation 2002; 105:823–829.
27. Shaw LJ, Hachamovitch R, Berman DS, et al. The economic consequences of available diagnostic and prognostic strategies for the evaluation of stable angina patients: an observational assessment of the value of precatheterization ischemia. Economics of Noninvasive Diagnosis (END) Multicenter Study Group. J Am Coll Cardiol 1999;33: 661–669.
28. Udelson JE, Beshansky JR, Ballin DS, et al. Myocardial perfusion imaging for evaluation and triage of patients with suspected acute cardiac ischemia: a randomized controlled trial. JAMA 2002;288:2693–2700.
29. Brown KA, Heller GV, Landin RS, et al. Early dipyridamole (99m)Tc-sestamibi single photon emission computed tomographic imaging 2 to 4 days after acute myocardial infarction predicts in-hospital and postdischarge cardiac events: comparison with submaximal exercise imaging. Circulation 1999;100:2060–2066.
30. Wackers FJ, Zaret BL. Detection of myocardial ischemia in patients with diabetes mellitus. Circulation 2002;105:5–7.
31. Leung DY, Dawson IG, Thomas JD, Marwick TH. Accuracy and cost-effectiveness of exercise echocardiography for detection of coronary artery disease in patients with mitral valve prolapse. Am Heart J 1997;134: 1052–1057.
32. Mairesse GH, Vanoverschelde JL, Robert A, Climov D, Detry JM, Marwick TH. Pathophysiologic mechanisms underlying dobutamine- and exercise-induced wall motion abnormalities. Am Heart J 1998;136:63–70.
33. Senior R, Lepper W, Pasquet A, et al. Myocardial perfusion assessment in patients with medium probability of coronary artery disease and no prior myocardial infarction: comparison of myocardial contrast echocardiography with 99mTc single-photon emission computed tomography. Am Heart J 2004;147:1100–1105.
34. Nagel E, Lehmkuhl HB, Bocksch W, et al. Noninvasive diagnosis of ischemia-induced wall motion abnormalities with the use of high-dose dobutamine stress MRI: comparison with dobutamine stress echocardiography. Circulation 1999;99:763–770.
35. Al-Saadi N, Nagel E, Gross M, et al. Noninvasive detection of myocardial ischemia from perfusion reserve based on cardiovascular magnetic resonance. Circulation 2000; 101:1379–1383.
36. Murry CE, Jennings RB, Reimer KA. Preconditioning with ischemia: a delay of lethal cell injury in ischemic myocardium. Circulation 1986;74:1124–1136.
37. Hofstra L, Liem IH, Dumont EA, et al. Visualisation of cell death in vivo in patients with acute myocardial infarction. Lancet 2000; 356:209–212.
38. Dumont EA, Hofstra L, van Heerde WL, et al. Cardiomyocyte death induced by myocardial ischemia and reperfusion: measurement with recombinant human annexin-V in a mouse model. Circulation 2000;102: 1564–1568.
39. Thimister PW, Hofstra L, Liem IH, et al. In vivo detection of cell death in the area at risk in acute myocardial infarction. J Nucl Med 2003;44:391–396.
40. Dilsizian V, Bateman TM, Bergmann SR, et al. Metabolic imaging with beta-methyl-p-[(123)I]-iodophenyl-pentadecanoic acid identifies ischemic memory after demand ischemia. Circulation 2005;112:2169–2174.
41. Bülow HP, Stahl F, Lauer B, et al. Alterations of myocardial presynaptic sympathetic innervation in patients with multi-vessel coronary artery disease but without history of myocardial infarction. Nucl Med Commun 2003;24:233–239.
42. Simoes MV, Barthel P, Matsunari I, et al. Presence of sympathetically denervated but viable myocardium and its electrophysiologic correlates after early revascularized acute myocardial infarction. Eur Heart J 2004;25:551–557.
43. Sakata K, Mochizuki M, Yoshida H, et al. Cardiac sympathetic dysfunction contributes to left ventricular remodeling after acute myocardial infarction. Eur J Nucl Med 2000;27:1641–1649.
44. Spyrou N, Rosen SD, Fath-Ordoubadi F, et al. Myocardial beta-adrenoceptor density one month after acute myocardial infarction predicts left ventricular volumes at six months. J Am Coll Cardiol 2002;40:1216–1224.
45. Meoli DF, Sadeghi MM, Krassilnikova S, et al. Noninvasive imaging of myocardial angiogenesis following experimental myocardial infarction. J Clin Invest 2004;113: 1684–1691.
46. Villanueva FS. Molecular images of neovascularization: art for art's sake or form with a function? Circulation 2005;111: 3188–3191.
47. Kaul TK, Agnihotri AK, Fields BL, Riggins LS, Wyatt DA, Jones CR. Coronary artery bypass grafting in patients with an ejection fraction of twenty percent or less. J Thorac Cardiovasc Surg 1996;111:1001–1012.
48. Miller DC, Stinson EB, Alderman EL. Surgical treatment of ischemic cardiomyopathy: is it ever too late? Am J Surg 1981;141:688–693.
49. Mickleborough LL, Maruyama H, Takagi Y, Mohammed S, Sun Z, Ebisuzaki L. Results of revascularization in patients with severe left ventricular dysfunction. Circulation 1995; 92(9 suppl):II73–II79.
50. Passamani E, Davis KB, Gillespie MJ, Killip T. A randomized trial of coronary artery bypass surgery: survival of patients with a low ejection fraction. N Engl J Med 1985; 312:1665–1671.
51. Rahimtoola SH. The hibernating myocardium. Am Heart J 1989;117:211–221.

52. Dyke SH, Cohn PF, Gorlin R, Sonnenblick EH. Detection of residual myocardial function in coronary artery disease using post-extra systolic potentiation. Circulation 1974; 50:694–699.

53. Diamond GA, Forrester JS, deLuz PL, Wyatt HL, Swan HJ. Post-extrasystolic potentiation of ischemic myocardium by atrial stimulation. Am Heart J 1978;95:204–209.

54. Bax JJ, Wijns W, Cornel JH, Visser FC, Boersma E, Fioretti PM. Accuracy of currently available techniques for prediction of functional recovery after revascularization in patients with left ventricular dysfunction due to chronic coronary artery disease: comparison of pooled data. J Am Coll Cardiol 1997;30:1451–1460.

55. Kloner RA, Bolli R, Marban E, Reinlib L, Braunwald E. Medical and cellular implications of stunning, hibernation, and preconditioning: an NHLBI Workshop. Circulation 1998;97:1848–1867.

56. Gao WD, Liu Y, Mellgren R, Marban E. Intrinsic myofilament alterations underlying the decreased contractility of stunned myocardium: a consequence of Ca2+-dependent proteolysis? Circ Res 1996;78:455–465.

57. Bolli R. Mechanism of myocardial stunning. Circulation 1990;82:723–736.

58. Heusch G. Hibernating myocardium. Physiol Rev 1998;78:1055–1085.

59. Elsässer A, Schlepper M, Klovekorn WP, et al. Hibernating myocardium: an incomplete adaptation to ischemia. Circulation 1997; 96:2920–2931.

60. Depre C, Vanoverschelde JL, Taegtmeyer H. Glucose for the heart. Circulation 1999; 99:578–588.

61. Schwarz ER, Schoendube FA, Kostin S, et al. Prolonged myocardial hibernation exacerbates cardiomyocyte degeneration and impairs recovery of function after revascularization. J Am Coll Cardiol 1998;31:1018–1026.

62. Schwaiger M, Fishbein MC, Block M, et al. Metabolic and ultrastructural abnormalities during ischemia in canine myocardium: noninvasive assessment by positron emission tomography. J Mol Cell Cardiol 1987;19: 259–269.

63. Tillisch J, Brunken R, Marshall R, et al. Reversibility of cardiac wall motion abnormalities predicted by positron tomography. N Engl J Med 1986;314:884–888.

64. Vanoverschelde JL, Wijns W, Depre C, et al. Mechanisms of chronic regional postischemic dysfunction in humans: new insights from the study of noninfarcted collateral-dependent myocardium. Circulation 1993; 87:1513–1523.

65. Schelbert HR, Beanlands R, Bengel F, et al. PET myocardial perfusion and glucose metabolism imaging. II. Guidelines for interpretation and reporting. J Nucl Cardiol 2003;10:557–571.

66. Bacharach SL, Bax JJ, Case J, et al. PET myocardial glucose metabolism and perfusion imaging. I. Guidelines for data acquisition and patient preparation. J Nucl Cardiol 2003;10:543–556.

67. Di Carli MF, Davidson M, Little R, et al. Value of metabolic imaging with positron emission tomography for evaluating prognosis in patients with coronary artery disease and left ventricular dysfunction. Am J Cardiol 1994;73:527–533.

68. Haas F, Haehnel CJ, Picker W, et al. Preoperative positron emission tomographic viability assessment and perioperative and postoperative risk in patients with advanced ischemic heart disease. J Am Coll Cardiol 1997;30:1693–1700.

69. Di Carli MF, Asgarzadie F, Schelbert HR, et al. Quantitative relation between myocardial viability and improvement in heart failure symptoms after revascularization in patients with ischemic cardiomyopathy. Circulation 1995;92:3436–3444.

70. Beanlands RS, Hendry PJ, Masters RG, deKemp RA, Woodend K, Ruddy TD. Delay in revascularization is associated with increased mortality rate in patients with severe left ventricular dysfunction and viable myocardium on fluorine 18-fluorodeoxyglucose positron emission tomography imaging. Circulation 1998;98(19 suppl):II51–II56.

71. Bax JJ, Valkema R, Visser FC, et al. FDG SPECT in the assessment of myocardial viability: comparison with dobutamine echo. Eur Heart J 1997;18(suppl D):D124–D129.

72. Klein C, Nekolla SG, Bengel FM, et al. Assessment of myocardial viability with contrast enhanced magnetic resonance imaging: comparison with positron emission tomography. Circulation 2002;105:162–167.

73. Haas F, Augustin N, Holper K, et al. Time course and extent of improvement of dysfunctioning myocardium in patients with coronary artery disease and severely depressed left ventricular function after revascularization: correlation with positron emission tomographic findings. J Am Coll Cardiol 2000;36:1927–1934.

74. Kim RJ, Wu E, Rafael A, et al. The use of contrast-enhanced magnetic resonance imaging to identify reversible myocardial dysfunction. N Engl J Med 2000;343:1445–1453.

75. Wellnhofer E, Olariu A, Klein C, et al. Magnetic resonance low-dose dobutamine test is superior to scar quantification for the prediction of functional recovery. Circulation 2004;109:2172–2174.

76. Hunt SA, Baker DW, Chin MH, et al. ACC/AHA guidelines for the evaluation and management of chronic heart failure in the adult: executive summary—a report of the American College of Cardiology/American Heart Association Task Force on Practice Guidelines (committee to revise the 1995 Guidelines for the Evaluation and Management of Heart Failure). J Am Coll Cardiol 2001;38: 2101–2113.

77. Massie BM, Shah NB. Evolving trends in the epidemiologic factors of heart failure: rationale for preventive strategies and comprehensive disease management. Am Heart J 1997;133:703–712.

78. Chen L, Hay JW. Cost-effectiveness of primary implanted cardioverter defibrillator for sudden death prevention in congestive heart failure. Cardiovasc Drugs Ther 2004; 18:161–170.

79. Haldeman GA, Croft JB, Giles WH, Rashidee A. Hospitalization of patients with heart failure: National Hospital Discharge Survey, 1985 to 1995. Am Heart J 1999; 137:352–360.

80. Farr MA, Basson CT. Sparking the failing heart. N Engl J Med 2004;351:185–187.

81. Moss AJ, Zareba W, Hall WJ, et al. Prophylactic implantation of a defibrillator in patients with myocardial infarction and reduced ejection fraction. N Engl J Med 2002; 346:877–883.

82. Boecker W, Bernecker OY, Wu JC, et al. Cardiac specific gene expression facilitated by an enhanced myosin light chain promoter. Mol Imaging 2004;3:69–75.

83. Baldasseroni S, Opasich C, Gorini M, et al. Left bundle-branch block is associated with increased 1-year sudden and total mortality rate in 5517 outpatients with congestive heart failure: a report from the Italian network on congestive heart failure. Am Heart J 2002;143:398–405.

84. Abraham WT, Fisher WG, Smith AL, et al. Cardiac resynchronization in chronic heart failure. N Engl J Med 2002;346:1845–1853.

85. Leclercq C, Kass DA. Retiming the failing heart: principles and current clinical status of cardiac resynchronization. J Am Coll Cardiol 2002;39:194–201.

86. Bax JJ, Molhoek SG, van Erven L, et al. Usefulness of myocardial tissue Doppler echocardiography to evaluate left ventricular dyssynchrony before and after biventricular pacing in patients with idiopathic dilated cardiomyopathy. Am J Cardiol 2003; 91:94–97.

87. Heimdal A, Stoylen A, Torp H, Skjaerpe T. Real-time strain rate imaging of the left ventricle by ultrasound. J Am Soc Echocardiogr 1998;11:1013–1019.

88. Breithardt OA, Stellbrink C, Herbots L, et al. Cardiac resynchronization therapy can reverse abnormal myocardial strain distribution in patients with heart failure and left bundle branch block. J Am Coll Cardiol 2003;42:486–494.

89. Bax JJ, Ansalone G, Breithardt OA, et al. Echocardiographic evaluation of cardiac resynchronization therapy: ready for routine clinical use? a critical appraisal. J Am Coll Cardiol 2004;44:1–9.

90. Sutherland GR, Di Salvo G, Claus P, D'Hooge J, Bijnens B. Strain and strain rate

imaging: a new clinical approach to quantifying regional myocardial function. J Am Soc Echocardiogr 2004;17:788–802.

91. Carrio I. Cardiac neurotransmission imaging. J Nucl Med 2001;42:1062–1076.

92. Henderson EB, Kahn JK, Corbett JR, et al. Abnormal I-123 metaiodobenzylguanidine myocardial washout and distribution may reflect myocardial adrenergic derangement in patients with congestive cardiomyopathy. Circulation 1988;78:1192–1199.

93. Schofer J, Spielmann R, Schuchert A, Weber K, Schluter M. Iodine-123 meta-iodobenzylguanidine scintigraphy: a noninvasive method to demonstrate myocardial adrenergic nervous system disintegrity in patients with idiopathic dilated cardiomyopathy. J Am Coll Cardiol 1988;12:1252–1258.

94. Arimoto T, Takeishi Y, Fukui A, et al. Dynamic 123I-MIBG SPECT reflects sympathetic nervous integrity and predicts clinical outcome in patients with chronic heart failure. Ann Nucl Med 2004;18:145–150.

95. Kyuma M, Nakata T, Hashimoto A, et al. Incremental prognostic implications of brain natriuretic peptide, cardiac sympathetic nerve innervation, and noncardiac disorders in patients with heart failure. J Nucl Med 2004;45:155–163.

96. Arora R, Ferrick KJ, Nakata T, et al. I-123 MIBG imaging and heart rate variability analysis to predict the need for an implantable cardioverter defibrillator. J Nucl Cardiol 2003;10:121–131.

97. Wu JC, Yla-Herttuala S. Human gene therapy and imaging: cardiology. Eur J Nucl Med Mol Imaging 2005;32(suppl 2):S346–S357.

98. Wu JC, Tseng JR, Gambhir SS. Molecular imaging of cardiovascular gene products. J Nucl Cardiol 2004;11:491–505.

99. Yla-Herttuala S, Alitalo K. Gene transfer as a tool to induce therapeutic vascular growth. Nat Med 2003;9:694–701.

100. Takeshita S, Pu LQ, Stein LA, et al. Intramuscular administration of vascular endothelial growth factor induces dose-dependent collateral artery augmentation in a rabbit model of chronic limb ischemia. Circulation 1994;90(5 pt 2):II228–II234.

101. Brogi E, Wu T, Namiki A, Isner JM. Indirect angiogenic cytokines upregulate VEGF and bFGF gene expression in vascular smooth muscle cells, whereas hypoxia upregulates VEGF expression only. Circulation 1994;90:649–652.

102. Shyu KG, Wang MT, Wang BW, et al. Intramyocardial injection of naked DNA encoding HIF-1alpha/VP16 hybrid to enhance angiogenesis in an acute myocardial infarction model in the rat. Cardiovasc Res 2002;54:576–583.

103. Steg PG, Tahlil O, Aubailly N, et al. Reduction of restenosis after angioplasty in an atheromatous rabbit model by suicide gene therapy. Circulation 1997;96:408–411.

104. Miyamoto MI, del Monte F, Schmidt U, et al. Adenoviral gene transfer of SERCA2a improves left-ventricular function in aortic-banded rats in transition to heart failure. Proc Natl Acad Sci U S A 2000;97:793–798.

105. Kozarsky KF, Donahee MH, Glick JM, Krieger M, Rader DJ. Gene transfer and hepatic overexpression of the HDL receptor SR-BI reduces atherosclerosis in the cholesterol-fed LDL receptor-deficient mouse. Arterioscler Thromb Vasc Biol 2000;20:721–727.

106. Matsui T, Li L, del Monte F, et al. Adenoviral gene transfer of activated phosphatidylinositol 3′-kinase and Akt inhibits apoptosis of hypoxic cardiomyocytes in vitro. Circulation 1999;100:2373–2379.

107. National Institutes of Health Office of Biotechnology Advances. Clinical trials in human gene transfer: query of clinical trials. http://www4.od.nih.gov/oba/rac/trialqueryform.asp. Accessed April 1, 2006.

108. Rosengart TK, Lee LY, Patel SR, et al. Angiogenesis gene therapy: phase I assessment of direct intramyocardial administration of an adenovirus vector expressing VEGF121 cDNA to individuals with clinically significant severe coronary artery disease. Circulation 1999;100:468–474.

109. Symes JF, Losordo DW, Vale PR, et al. Gene therapy with vascular endothelial growth factor for inoperable coronary artery disease. Ann Thorac Surg 1999;68:830–836.

110. Vale PR, Losordo DW, Milliken CE, et al. Left ventricular electromechanical mapping to assess efficacy of phVEGF(165) gene transfer for therapeutic angiogenesis in chronic myocardial ischemia. Circulation 2000;102:965–974.

111. Henry TD, Annex BH, McKendall GR, et al. The VIVA trial: vascular endothelial growth factor in ischemia for vascular angiogenesis. Circulation 2003;107:1359–1365.

112. Simons M, Annex BH, Laham RJ, et al. Pharmacological treatment of coronary artery disease with recombinant fibroblast growth factor-2: double-blind, randomized, controlled clinical trial. Circulation 2002;105:788–793.

113. Grines CL, Watkins MW, Mahmarian JJ, et al. A randomized, double-blind, placebo-controlled trial of Ad5FGF-4 gene therapy and its effect on myocardial perfusion in patients with stable angina. J Am Coll Cardiol 2003;42:1339–1347.

114. Grines CL, Watkins MW, Helmer G, et al. Angiogenic Gene Therapy (AGENT) trial in patients with stable angina pectoris. Circulation 2002;105:1291–1297.

115. Hedman M, Hartikainen J, Syvanne M, et al. Safety and feasibility of catheter-based local intracoronary vascular endothelial growth factor gene transfer in the prevention of postangioplasty and in-stent restenosis and in the treatment of chronic myocardial ischemia: phase II results of the Kuopio Angiogenesis Trial (KAT). Circulation 2003;107:2677–2683.

116. Pislaru S, Janssens SP, Gersh BJ, Simari RD. Defining gene transfer before expecting gene therapy: putting the horse before the cart. Circulation 2002;106:631–636.

117. Tjuvajev JG, Finn R, Watanabe K, et al. Noninvasive imaging of herpes virus thymidine kinase gene transfer and expression: a potential method for monitoring clinical gene therapy. Cancer Res 1996;56:4087–4095.

118. Gambhir SS, Barrio JR, Wu L, et al. Imaging of adenoviral-directed herpes simplex virus type 1 thymidine kinase reporter gene expression in mice with radiolabeled ganciclovir. J Nucl Med 1998;39:2003–2011.

119. Wu JC, Inubushi M, Sundaresan G, Schelbert HR, Gambhir SS. Positron emission tomography imaging of cardiac reporter gene expression in living rats. Circulation 2002;106:180–183.

120. Wu JC, Inubushi M, Sundaresan G, Schelbert HR, Gambhir SS. Optical imaging of cardiac reporter gene expression in living rats. Circulation 2002;105:1631–1634.

121. Inubushi M, Wu JC, Gambhir SS, et al. Positron-emission tomography reporter gene expression imaging in rat myocardium. Circulation 2003;107:326–332.

122. Bengel FM, Anton M, Richter T, et al. Noninvasive imaging of transgene expression by use of positron emission tomography in a pig model of myocardial gene transfer. Circulation 2003;108:2127–2133.

123. Chen IY, Wu JC, Min JJ, et al. Micropositron emission tomography imaging of cardiac gene expression in rats using bicistronic adenoviral vector-mediated gene delivery. Circulation 2004;109:1415–1420.

124. Wu JC, Chen IY, Wang Y, et al. Molecular imaging of the kinetics of vascular endothelial growth factor gene expression in ischemic myocardium. Circulation 2004;110:685–691.

125. Anton M, Wittermann C, Haubner R, et al. Coexpression of herpesviral thymidine kinase reporter gene and VEGF gene for noninvasive monitoring of therapeutic gene transfer: an in vitro evaluation. J Nucl Med 2004;45:1743–1746.

126. Bouchard S, MacKenzie TC, Radu AP, et al. Long-term transgene expression in cardiac and skeletal muscle following fetal administration of adenoviral or adeno-associated viral vectors in mice. J Gene Med 2003;5:941–950.

127. Askari A, Unzek S, Goldman CK, et al. Cellular, but not direct, adenoviral delivery of vascular endothelial growth factor results in improved left ventricular function and neovascularization in dilated ischemic cardiomyopathy. J Am Coll Cardiol 2004;43:1908–1914.

128. Orlic D, Kajstura J, Chimenti S, et al. Bone marrow cells regenerate infarcted myocardium. Nature 2001;410:701–705.

129. Nygren JM, Jovinge S, Breitbach M, et al.

Bone marrow-derived hematopoietic cells generate cardiomyocytes at a low frequency through cell fusion, but not transdifferentiation. Nat Med 2004;10:494–501.

130. Murry CE, Soonpaa MH, Reinecke H, et al. Haematopoietic stem cells do not transdifferentiate into cardiac myocytes in myocardial infarcts. Nature 2004;428:664–668.

131. Strauer BE, Brehm M, Zeus T, et al. Repair of infarcted myocardium by autologous intracoronary mononuclear bone marrow cell transplantation in humans. Circulation 2002;106:1913–1918.

132. Assmus B, Schachinger V, Teupe C, et al. Transplantation of progenitor cells and regeneration enhancement in acute myocardial infarction (TOPCARE-AMI). Circulation 2002;106:3009–3017.

133. Menasche P, Hagege AA, Vilquin JT, et al. Autologous skeletal myoblast transplantation for severe postinfarction left ventricular dysfunction. J Am Coll Cardiol 2003;41:1078–1083.

134. Pagani FD, DerSimonian H, Zawadzka A, et al. Autologous skeletal myoblasts transplanted to ischemia-damaged myocardium in humans. Histological analysis of cell survival and differentiation. J Am Coll Cardiol 2003;41:879–888.

135. Tse HF, Kwong YL, Chan JK, Lo G, Ho CL, Lau CP. Angiogenesis in ischaemic myocardium by intramyocardial autologous bone marrow mononuclear cell implantation. Lancet 2003;361:47–49.

136. Perin EC, Dohmann HF, Borojevic R, et al. Transendocardial, autologous bone marrow cell transplantation for severe, chronic ischemic heart failure. Circulation 2003;107:2294–2302.

137. Stamm C, Kleine HD, Westphal B, et al. CABG and bone marrow stem cell transplantation after myocardial infarction. Thorac Cardiovasc Surg 2004;52:152–158.

138. Wollert KC, Meyer GP, Lotz J, et al. Intracoronary autologous bone-marrow cell transfer after myocardial infarction: the BOOST randomised controlled clinical trial. Lancet 2004;364:141–148.

139. Meyer GP, Wollert KC, Lotz J, et al. Intracoronary bone marrow cell transfer after myocardial infarction: eighteen months' follow-up data from the randomized, controlled BOOST (BOne marrOw transfer to enhance ST-elevation infarct regeneration) trial. Circulation 2006;113:1287–1294.

140. Reinlib L, Field L. Cell transplantation as future therapy for cardiovascular disease? a workshop of the National Heart, Lung, and Blood Institute. Circulation 2000;101:E182–E187.

141. Aicher A, Brenner W, Zuhayra M, et al. Assessment of the tissue distribution of transplanted human endothelial progenitor cells by radioactive labeling. Circulation 2003;107:2134–2139.

142. Kraitchman DL, Heldman AW, Atalar E, et al. In vivo magnetic resonance imaging of mesenchymal stem cells in myocardial infarction. Circulation 2003;107:2290–2293.

143. Wu JC, Chen IY, Sundaresan G, et al. Molecular imaging of cardiac cell transplantation in living animals using optical bioluminescence and positron emission tomography. Circulation 2003;108:1302–1305.

144. Murry CE, Wiseman RW, Schwartz SM, Hauschka SD. Skeletal myoblast transplantation for repair of myocardial necrosis. J Clin Invest 1996;98:2512–2523.

145. Zhang M, Methot D, Poppa V, Fujio Y, Walsh K, Murry CE. Cardiomyocyte grafting for cardiac repair: graft cell death and anti-death strategies. J Mol Cell Cardiol 2001;33:907–921.

146. Muller-Ehmsen J, Whittaker P, Kloner RA, et al. Survival and development of neonatal rat cardiomyocytes transplanted into adult myocardium. J Mol Cell Cardiol 2002;34:107–116.

147. Cao F, Lin S, Xie X, et al. In vivo visualization of embryonic stem cell survival, proliferation, and migration after cardiac delivery. Circulation 2006;113:1005–1014.

148. Wu JC, Spin JM, Cao F, et al. Transcriptional profiling of reporter genes used for molecular imaging of embryonic stem cell transplantation. Physiol Genomics 2006;25:29–38.

149. Reinecke H, Murry CE. Taking the death toll after cardiomyocyte grafting: a reminder of the importance of quantitative biology. J Mol Cell Cardiol 2002;34:251–253.

150. Mangi AA, Noiseux N, Kong D, et al. Mesenchymal stem cells modified with Akt prevent remodeling and restore performance of infarcted hearts. Nat Med 2003;9:1195–1201.

151. Gheysens O, Lin S, Cao F, et al. Noninvasive evaluation of immunosuppressive drug efficacy on acute donor cell survival. Mol Imaging Biol 2006;8:163–170.

152. Sheikh AY, Wu JC. Molecular imaging of cardiac stem cell transplantation. Curr Cardiol Rep 2006;8:147–154.